SNOW ROAD CONSTRUCTION

A THESIS
SUBMITTED TO THE
FACULTY OF GRADUATE STUDIES
UNIVERSITY OF MANITOBA
IN PARTIAL FULFILMENT OF THE REQUIREMENTS FOR THE
DEGREE MASTER OF SCIENCE IN CIVIL ENGINEERING

by

MICHAEL ZENON KOWALCHUK

Winnipeg, Manitoba
December 1976

"SNOW ROAD CONSTRUCTION"

by

MICHAEL ZENNON KOWALCHUK

A dissertation submitted to the Faculty of Graduate Studies of the University of Manitoba in partial fulfillment of the requirements of the degree of

MASTER OF SCIENCE

ABSTRACT

This study investigates the application of snow in the construction of snow roads and the suitability of the snow road as a transportation facility. The snow properties are reviewed and the current status of snow road technology is identified. In the field studies, where variations in snow road construction procedures are evaluated, a conventional snow blower is utilized as a snow processing implement. The results indicate that an equidimensional particle size is produced with no significant change occuring in either the particle size or distribution with repeated processing. The results further identify the operational difficulties in handling blower-processed snow during snow road construction. Increasing the snow road density by introduction of free moisture into the pore spaces, through surface heat application, is also investigated. For this purpose a prototype wood-fired heater is utilized. The test results give promising indication that this method of surface heat application, in combination with heavy compaction, could have considerable practical merit. The snow road strength is indicated in terms of snow 'hardness' determined by the Rammsonde cone penetrometer. The conventional Rammsonde hardness equation is re-evaluated and the hardness index is correlated to snow temperature.

ACKNOWLEDGEMENTS

I wish to express my sincere appreciation and gratitude to Dr. K.M. Adam for his guidance and assistance in the preparation of this thesis and for his generous and unstinting help during all phases of the degree program. Sincere appreciation is also extended to the members of the thesis examination committee, Dr. J. Graham and Dr. G.E. Laliberte, for their invaluable suggestions.

I give full acknowledgement of my indebtedness to the University of Manitoba Maintenance Department for making available, on a rental basis, the necessary equipment and personnel, and to the National Research Council of Canada who provided financial support for the project. I also gratefully acknowledge the personal sources of assistance which during the course of the degree program included: a University of Manitoba Graduate Research Assistantship, a University of Manitoba Graduate Fellowship, and a National Research Council Post-graduate Scholarship.

To Ms. Janet Gourlay, I extend my warmest thanks for doing a fine job in typing this manuscript and for offering timely editorial advice.

Finally, I wish to express my deepest gratitude to my parents for instilling in me the value of education that has guided my endeavours.

TABLE OF CONTENTS

Chapter		Page
	ABSTRACT	i.
	ACKNOWLEDGEMENTS	ii.
	TABLE OF CONTENTS	iii.
	LIST OF TABLES	vii.
	LIST OF FIGURES	viii.
	LIST OF PHOTOGRAPHS	x.
	LIST OF SYMBOLS	xi.
I	INTRODUCTION	1.
II	SNOW AS A MATERIAL	3.
	A. SNOW METAMORPHISM	3.
	Destructive Metamorphism	3.
	Constructive Metamorphism	4.
	Melt Metamorphism	4.
	Pressure Metamorphism	5.
	B. SNOW AS A POROUS MEDIUM	7.
	Porosity	7.
	Pore-size Distribution	8.
	Bubbling Pressure	9.
	Saturated Permeability and Conductivity	10.
	Relative Permeability and Saturation Relationships	13.
	C. WATER FLOW THROUGH SNOW	17.
	General Flow Equations	17.
	Capillary-pressure, Saturation Relationships	20.

Chapter		Page
	D. HEAT AND MASS TRANSFER	22.
	E. SNOW MECHANICS	27.
	Densification	27.
	Response to Rapid Loading	28.
	Response to Sustained Loading	31.
	F. INDEX PROPERTIES	34.
	Density	34.
	Grain Size	34.
	Grain Shape	36.
	Temperature	37.
	Hardness	37.
III	WINTER ROADS	43.
	System of Classification	43.
	Route Selection	44.
	Measures to Increase the Bearing Capacity of Snow	45.
	A. SNOW ROAD CONSTRUCTION	46.
	Initial Site Preparation	46.
	Disaggregation/Processing	46.
	Leveling-Compacting	47.
	Preparing Final Surface	47.
	B. CONSTRUCTION METHODS AND RESULTS	49.
	The Scandinavian Experience	49.
	The North American Experience	52.
	1. Camp Hale, Colorado	52.
	2. Point Barrow, Alaska	53.
	3. Churchill, Manitoba	56.

Chapter		Page
	4. Greenland	58.
	5. Kapuskasing, Ontario	63.
	6. McMurdo Station, Antarctica	66.
	7. Norman Wells, N.W.T.	68.
IV	FIELD STUDIES	73.
	A. EXPERIMENTAL TECHNIQUES	73.
	Construction of Snow Road Test Lanes	73.
	Surface Compaction at 0°C	74.
	Rammsonde Hardness Tests	74.
	Temperature	75.
	Grain Size	75.
	Density	76.
	The Prototype Wood-fired Surface Heater	76.
	B. RESULTS AND DISCUSSION	78.
	Construction of Test Lanes	78.
	Porosity, Density and Grain Size	79.
	Performance Characteristics of the Sicard Snow Blower	81.
	Rammsonde Hardness of Test Lanes	81.
	Rammsonde Hardness - Temperature Relationships	82.
	Burn Tests	83.
V	CONCLUSIONS AND RECOMMENDATIONS	85.
	BIBLIOGRAPHY	88.
	APPENDIX A	A.1
	RAMMSONDE HARDNESS DATA AND OBSERVATIONS	

	Page
APPENDIX B	B.1
EXPERIMENTAL RESULTS FROM BURN TESTS	
APPENDIX C	C.1
THE RAMMSONDE CONE PENETROMETER	
APPENDIX D	D.1
DETERMINATION OF SNOW DENSITY USING A RADIATION MEASUREMENT TECHNIQUE	
APPENDIX E	E.1
CONSTRUCTION EQUIPMENT AND MATERIALS	

LIST OF TABLES

Table		Page
2-1	Effective thermal conductivity (K_e) of dry snow.	24.
2-2	Snow Classification.	35.
2-3	Summary of regression and correlation coefficients.	41.
3-1	Summary of traffic tests.	65.
A-1	Summary of Rammsonde test results.	A.2
A-2	Summary of air temperature, snow road temperature and relative humidity for duration of Rammsonde testing.	A.16
A-3	Average densities of single- and multiple-processed snow roads.	A.26
B-1	Summary of snow road density profiles before burn tests.	B.2
B-2	Summary of snow road density profiles after burn tests.	B.3

LIST OF FIGURES

Figure		Page
2-1	Capillary pressure as a function of liquid saturation.	20.
2-2	Relationship between dynamic Young's modulus and snow density.	28.
2-3	Unconfined compressive strength versus density for naturally compacted snow.	30.
2-4	Tensile strength of high density snow at a temperature of - 10°C.	30.
2-5	Strength in double shear plotted against density.	30.
2-6	Required ram hardness for supporting various wheel loads.	38.
2-7	Required hardness (or strength) of a snow pavement for various wheel load conditions.	39.
2-8	Average tensile strength as a function of ram resistance and age.	40.
3-1	Normal hardness growth in a single layer of polar snow.	60.
3-2	Typical vertical hardness in compacted snow compared with its redistribution after surface hardening.	61.
3-3	Tentative minimum hardness guide for compacted snow runways on deep snow.	62.
A-1	Typical snow road hardness profiles as indicated by the corrected and uncorrected versions of the Rammsonde hardness data.	A.15
A-2	Relationship between Rammsonde hardness, age-hardening time and air temperature.	A.23
A-3	Scatter diagram of Rammsonde hardness and snow road temperature data.	A.25

LIST OF FIGURES (cont'd)

Figure		Page
A-4	Typical snow road hardness increase due to surface compaction at 0°C.	A.27
B-1	Snow road density profiles before and after burn tests.	B.5
C-1	Diagram of Rammsonde cone penetrometer showing the components of the instrument.	C.2
D-1	Diagram showing the arrangement and basic components of the radiation/scintillation apparatus.	D.7
E-1	Diagram showing the construction of the prototype wood-fired surface heater.	E.5

LIST OF PHOTOGRAPHS

Photograph		Page
E-1	Windrowing the snow with the Champion Motor grader in preparation for processing with the Sicard snowblower	E.6
E-2	A view of the snowblower/tractor unit processing the windrowed snow and depositing it along the proposed roadway	E.6
E-3	The roadway after final snow processing and deposition	E.7
E-4	Road surface after leveling and dragging with the steel drag	E.7
E-5	Station-wagon traveling on the snow road with no detrimental effect on the road surface	E.8
E-6	The Champion motor grader blading minor snow accumulation from the snow road surface	E.8
E-7	The prototype surface heater fully fueled with one (1) cord of seasoned pine	E.9
E-8	A view of the surface heater in operation	E.9

LIST OF SYMBOLS

Symbol		Dimensions†
A	Empirical constant in strain-rate equation	none
a	Subscript indicating "air"	none
a	Subscript indicating "apparent"	none
a	Empirical constant in equation for hydraulic conductivity	none
b	Empirical constant in creep-rate equation	none
b	Subscript indicating "bubbling"	none
C	Hydraulic conductivity	L/t
C	Specific heat capacity	H/MT
C	Vapour concentration	M/L^3
C	Volumetric heat capacity	H/L^3T
C	Correction factor for effective conductivity	none
c	Subscript indicating "critical saturation"	none
c	Coefficient of cohesion	F/L^2
c	Subscript indicating "capillary"	none
D	Diffusivity	L^2/T
d	Grain diameter	L
E	Young's Modulus	F/L^2
e	Subscript indicating "effective"	none
e	Coefficient of restitution	none
e	Efficiency	none
g	Gravitational acceleration	L/t^2
H	Vertical distance	L
i	A counting integer	none

LIST OF SYMBOLS (cont'd)

Symbol		Dimensions*
i	Subscript indicating "ice"	none
K	Thermal conductivity	H/LTt
k	Permeability	L^2
k	A measure of confidence in units of "number of standard deviations"	
L	Latent heat of fusion	H/M
L	Characteristic length	L
l	Subscript indicating "liquid"	none
m	Mass	M
N	Empirical constant in equation for hydraulic conductivity	none
n	A counting integer	none
o	Subscript indicating "saturated"	none
P	Pressure	F/L^2
p	Subscript indicating "constant pressure"	none
Q	Weight of cone penetrometer	F
q	Intensity of evaporation or condensation	M/L^3t
q	Heat flux	H/L^2t
R	Rammsonde hardness number	F
r	Correlation coefficient	none
r	Subscript indicating "relative permeability"	none
r	Subscript indicating "residual"	none
S	Saturation	none
S	Penetration	L
s	Subscript indicating "solid"	none

Symbol		Dimensions†
s	Subscript indicating "snow"	none
s	Specific surface	L^2/L^3
s	Shear strength	F/L^2
T	Temperature	T
T	Detector resolution time	t
t	Time	t
V	Velocity	L/t
W	Weight	F
w	Subscript indicating "wetting phase"	none
x	Cone penetration	L
x	Spatial coordinate	L
z	Spatial coordinate	L
α	Thermal diffusivity	L^2/t
γ	Weight density	F/L^3
Δ	Denotes a difference	none
ε	Exponent in relative permeability equation	none
$\dot{\varepsilon}$	Strain-rate	t^{-1}
θ	Volumetric water content	L^3/L^3
λ	Pore-size distribution index; $-d(\log S_e)/d(\log P_c)$	none
μ	Dynamic viscosity	Ft/L^2
ν	Poisson's ratio	L/L
ρ	Mass density	M/L^3
Σ	Summation	none

LIST OF SYMBOLS (cont'd)

Symbol		Dimensions†
σ	Stress	F/L^2
ϕ	Porosity	none
ϕ	Angle of shearing resistance	none
∇	Gradient operator	$1/L$
div	Divergence operator	$1/L$
*	Superscript indicating resultant of surface and body forces	none

† Fundamental dimensions: force ....F
heat ....H
length L
mass ....M
temperature ....T
time ....t

CHAPTER I

INTRODUCTION

With increasing oil and gas exploration and the subsequent interest generated by this activity in Canada's North, the potential damage resulting from the movement of goods and machines becomes increasingly important. In particular, consideration of a Northern pipeline development has brought to the forefront a recognition of many multi-disciplinary problems.

The studies by Adam [1,2] point out the applicability of snow roads and ice-capped snow roads in the transportation of men and materials during winter pipeline construction. The studies also indicate that while the idea of compacting snow as a means of improving oversnow trafficability is extremely old, the procedure for constructing snow pavements capable of carrying heavy wheeled traffic, is not well established. This is partly due to the fact that in the past no apparent standard for the identification and treatment of the snow properties has been followed and that the existing information, though extensive, is widely dispersed.

In Chapter II and III of this study, pertinent facts are "pooled" to form a single comprehensive review. The review includes discussion of the porous characteristics and the thermodynamic and mechanical behaviour of snow. A procedural guide for the field identification of the index properties is also presented. Chapter III is a summary of the snow road construction experience where construction equipment, procedures and results are discussed.

Previous studies indicate that snow compaction alone will not produce the strength required of snow roads subjected to intensive wheeled traffic. Disaggregation, milling and mixing of the snow (prior to final grading and compaction), to produce a more non-uniform particle-size distribution becomes necessary. For this purpose, modified agricultural earth tillers and special pulvimixers have been used, but with varied success. In this study, the conventional snow blower is evaluated as a snow processing implement and the significance of multiple processing is determined.

The ice-capped snow road is a processed and compacted snowbed with water applied to the surface to increase the road density and strength. Although this class of winter road offers some significant advantages, its use may be seriously limited in permafrost regions where the large quantities of fresh water required may not be available. The feasibility of utilizing a portable wood-fired surface heater to produce the free water is investigated as an alternative to the direct water application method. The wood burner would have the dual advantage of utilizing right-of-way slash material as fuel , and at the same time provide a facility for the disposal of the waste material.

CHAPTER II

SNOW AS A MATERIAL

Snow is a porous medium composed of ice crystals and/or aggregates of ice grains. The pore spaces contain air, and water vapour and, in the case of "wet" snow, liquid water as well. Thus the snow pack forms a heterogeneous system which exhibits a complex and continuous interaction between the phases.

In this chapter, the properties of snow and the processes that occur due to the thermodynamic instability of snow are reviewed. The review cites pertinent theory and includes qualitative explanation of governing principles and terminology.

A. SNOW METAMORPHISM

Destructive Metamorphism

After the deposition of fresh snow, very local transformations, called destructive or isothermal metamorphism, are first observed. During this process the sharp points of the branches of individual snow flakes become blunt. This is achieved partly by evaporation due to the higher vapour pressures associated with small radii of curvature, and partly by the migration of molecules in the quasi-liquid surface layer (Bader [6]). The crystals become rounded and the larger spheres then grow at the expense of the smaller ones exclusively by vapour transfer. After a few days, crystal shape is almost completely lost. Each grain is a single crystal ranging from 0.5 to 1 mm in size with only one or two small crystallographic faces. The grains are weakly bonded and the density of this fine-grained snow usually ranges from 0.15 to 0.25 gm/cm^3.

Constructive Metamorphism

Following the original deposition of snow, a temperature gradient through the snow cover develops (colder at the top than at the bottom), and constructive or gradient metamorphism sets in. Constructive metamorphism involves heat and mass transfer and is characterized by growth of selected crystals; decrease of crystal number per unit bulk volume; and development of crystallographic faces, edges and vertices (de Quervain [18]). In dry snow, the mass transfer occurs primarily over the vapour phase by diffusion and,owing to the temperature gradient, is accelerated by convective air flow in the pore spaces.

At low snow densities (below 0.3 gm/cm^3), constructive metamorphism is very rapid and results in production of a distinctive snow type known as "depth hoar". Here grain size is between 2 and 8 mm and single crystals as large as 15 mm have been observed (Bader [2]). Depth hoar exhibits very poor bonding, and has a high viscosity. It is the major cause of avalanching and is most difficult to compact to a hard snow pavement.

Melt Metamorphism

Melt metamorphism characterizes the changes produced in snow by the presence of liquid water. As the weather becomes warmer, and the snow becomes moist, temperature gradients and their effect vanish (Yen [44]). Crystallographic elements also quickly vanish due to the high surface tension of the water film covering all the grains. Thus crystals become rounded and clusters of grains coalesce to form larger polycrystalline grains. As meltwater percolates through the snow, crystals grow to a maximum size of about 3 mm and composite grains to about 15 mm. The bonding between the grains is very weak and within a few days, the well known "rotten" snow of the thaw season is produced. Upon refreezing however, the wet snow aquires a high strength due to the growth in bond area.

Due to the inhomogeniety of the snow pack, the percolating meltwater is not equally distributed in all the layers. Some layers retain very little water while others absorb water almost to saturation which convert to dense ice lenses on refreezing.

Pressure Metamorphism

Pressure metamorphism characterizes the densification of dry nevé (granulated snow accumulated and subsequently compacted to glacier ice). This process is very slow and may take several decades to change snow of density 0.45 gm/cm^3 to ice of density 0.83 gm/cm^3. (At the density of 0.83 gm/cm^3, air permeability decreases to zero and the snow changes to ice by definition. Pure ice has a density of 0.917 gm/cm^3). During this period of slow change, grain and grain-bond growth by vapour or surface migration appears to be of secondary importance (Bader [6]). The densification is apparently dominated by processes of mechanical deformation under pressure.

At the surface of the snow pack, hard crusts generally form.

Bader [6] attributes crust formation to: refreezing of surface layers previously wetted by thaw, rainfall or wet fog fall-out, surface condensation from moist air, wind packing, and vapour migration from lower snow layers.

B. SNOW AS A POROUS MEDIUM

The parameters predominantly used to describe porous media systems are porosity, the pore-size distribution, and the relationships between capillary pressure and the permeability and saturation of the fluid phases. In treating snow systems (wet or dry), complications arise due to the inherent thermodynamic instability of snow. As evidenced earlier in the discussion of snow metamorphism the physical properties of snow are very strongly time and temperature dependent. Phase equilibrium and thermal complications prevent extensive experimental analysis of the parameters.

Porosity

Porosity is the ratio of volume of voids to the snow bulk volume. It is calculated from the measured snow density using the following relationship;

$$\phi = \frac{\rho_i - \rho_s}{\rho_i} = \frac{0.917 - \rho_s}{0.917} = 1 - 1.090\,\rho_s \qquad (2.1)$$

where

ϕ = porosity (sometimes called "absolute" porosity),

ρ_i = density of pure ice = 0.917 gm/cm^3,

ρ_s = density of snow, gm/cm^3.

The term "absolute" porosity is used when dealing with high-density snow (above 0.7 gm/cm^3) and is distinguished from "relative porosity" which refers to the volume of communicating pores only. Apparently at densities greater than 0.7 gm/cm^3, the volume of the isolated pores becomes significant. The relative and absolute porosities are approximately equal for low and medium density snow. No measurement of relative porosity of high-density snow was found in the review of pertinent literature.

Pore-Size Distribution

The hydraulic behaviour of a porous medium is affected by the porosity and the distribution of pore-sizes from point to point in the pore space. The pore-size distribution index, λ, is derived from a log-log plot of effective saturation S_e, versus capillary pressure head expressed as $P_c/\rho g$, (Laliberte [25]). The negative slope of the straight line portion of the curve represents the pore-size distribution index, λ. Qualitatively, the larger the index the more uniform is the pore-size distribution. Capillary pressure for the air-water system is defined as the pressure difference across the interface of the two immiscible fluids, given as

$$P_c = P_a - P_w \tag{2.2}$$

where

P_c = capillary pressure, dynes/cm^2, and

P_a, P_w = pressure of the air and water phases respectively, dynes/cm^2.

Effective saturation, S_e, is defined by;

$$S_e = \frac{S - S_r}{1 - S_r} \tag{2.3}$$

where

S = saturation, (volume of water expressed as a decimal fraction of the volume of voids), and

S_r = residual saturation, (saturation corresponding to a capillary pressure at which the saturation decreases very little with large increases in capillary pressure).

Friesen [22] obtained values of λ ranging from 6.2 to 9.9 for snow densities between 0.40 and 0.48 gm/cm^3. Colbeck (noted by Adam and Wilson [3]) obtained $\lambda = 4.9$ for snow densities of 0.55 and 0.59 gm/cm^3. Laliberte [25] indicates a pore-size distribution index of 7.3 for glass beads (uniform pore size) and 3.7 for a fine sand.

Bubbling Pressure

The bubbling pressure head, $P_b/\rho g$, is defined as the intercept of the straight line in the log-log plot of S_e versus $P_c/\rho g$, (Laliberte [25]). The bubbling pressure is a function of the largest continuous pores of the porous medium and is normally very close to the minimum capillary pressure head where the non-wetting fluid permeability can be measured during drainage. The lower the bubbling pressure, the larger are the continuous pores in the porous medium.

Colbeck (noted by Adam and Wilson [3]) obtained a bubbling pressure head of 5 cm for a snow-kerosene system and 3.7 cm for a snow-water system. Friesen [22] estimated a bubbling pressure head of 8 cm and 9 cm for snow densities of 0.48 gm/cm^3 and 0.40 gm/cm^3 respectively, in snow-soltrol C* systems.

Saturated Permeability and Conductivity

Fluid permeability is one of the basic quantities that describe the physical properties of a porous medium . Saturated "permeability" is distinguished from saturated "conductivity" the former being a quantity dependent on the porous matrix and the latter being a quantity dependent on the porous matrix and the fluid.

The relationship between volume flux and conductivity (for stable porous materials fully saturated with one liquid at a constant temperature) was discovered experimentally by D'Arcy. A popular form of the Darcy equation for one-dimensional flow is:

$$q = -C \frac{\Delta(\frac{p^*}{\rho g})}{L} \tag{2.4}$$

where

C = conductivity, cm/sec ,

p^* = piezometric potential, dynes/cm^2 (represents the resultant of the normal surface and body forces per unit volume acting on a volume element in a fluid of uniform density and has dimensions of energy per unit volume),

ρg = specific weight, dynes/cm^3,

$\frac{p^*}{\rho g}$ = piezometric head, cm ,

L = length over which the incremental change in piezometric head occurs in the direction of flow, cm , and

---

* Soltrol C is a light hydrocarbon oil.

q = volume flux, cm/sec (the component of the volume of discharge per unit time per unit of bulk area in the direction L).

The Darcy equation re-written in terms of permeability becomes

$$q = -\frac{K\,\Delta p^*}{\mu\,L} \tag{2.5}$$

where

μ = dynamic viscosity of the fluid, $\frac{\text{dyne-sec}}{\text{cm}^2}$, and
K = permeability, cm^2.

The coefficients C and K are related by

$$C = K\,\frac{\rho g}{\mu}. \tag{2.6}$$

Calculations of permeability and conductivity based on structural parameters have been proposed by various authors. The Kozeny-Carman equation (Laliberte [25]) approximates the saturated permeability of a porous medium with uniform pore size and low eccentricity:

$$K_{ow} = \frac{\phi^3}{5s^2} \tag{2.7}$$

where

K_{ow} = saturated permeability, cm^2 (permeability of the wetting phase at saturation $S = 1$),

ϕ = porosity, dimensionless, and

s = specific surface, cm^2/cm^3, (ratio of the surface area of solid pore boundaries to the bulk volume of the medium).

The equation yields poor approximations, however, for media exhibiting secondary porosity. Although snow usually possesses a small range of pore size, it exhibits some secondary porosity or structure.

Shimizu (Colbeck [11]) related the saturated permeability of snow to grain size and density by:

$$K_{ow} = 7.7 \times 10^{-4} d^2 \exp(-7.8 \times 10^{-3} \rho_s) \qquad (2.8)$$

where

d = grain diameter, cm , and

ρ_s = snow density, gm/cm^3 .

Kuriowa (Colbeck [10]) expresses the permeability of snow as a function of porosity:

$$K_{ow} = 1.17 \times 10^{-9} \exp(15.9\phi) \text{ cm}^2 \qquad (2.9)$$

For a snow-kerosene system, Kuriowa [24] relates saturated conductivity to porosity as follows:

$$C_{ow} = \frac{a\,\phi\,N}{N-\phi} \qquad (2.10)$$

where

C_{ow} = saturated conductivity cm/sec , and

a,N = emperical constants dependent on snow structure.

For snow-water systems, Moskalev (noted by de Quervain [18]) expresses saturated conductivity as a function of both porosity and grain size by the relationship:

$$C_{ow} = 2.88\ \phi\ d^{1.63}\ \text{cm/sec.} \tag{2.11}$$

where

d = mean grain diameter, mm .

de Quervain [18] obtained the following values of saturated conductivity for water in snow.

Grain Size	Snow Density (gm/cm^3)	C_{ow} (cm/sec)
$d < 1$ mm	0.35	0.57
$0.8 < d < 1.5$ mm	0.38	1.20
$d > 2$ mm	0.385	2.24

Colbeck and Davidson (summarized by Adam and Wilson [3]) observed the following permeabilities during water percolation in snow.

Snow Density (gm/cm^3)	Porosity (ϕ)	k_{ow} (cm^2)
0.653	0.32	1.2×10^{-6}
0.623	0.36	3.2×10^{-6}

Relative Permeability and Saturation Relationships

The concept of relative permeability has been applied extensively in dealing with porous media systems. The relative permeability of the wetting phase, k_{rw}, is defined by the ratio:

$$k_{rw} = \frac{k_w}{k_{ow}} \tag{2.12}$$

where

k_w = effective peremability, cm^2, (permeability of the wetting phase at a particular saturation S), and

k_{ow} = saturated permeability, cm^2, (permeability of the wetting phase at saturation $S = 1$).

Similarly, the relative permeability of the non-wetting phase, k_{rnw}, is defined by the ratio

$$k_{rnw} = \frac{k_{nw}}{k_{onw}} \tag{2.13}$$

where k_{onw} is the permeability to the non-wetting phase at saturation $S = 0$. Note that the subsctipts w and nw refer to the wetting and non-wetting phases respectively.

The relationship between relative permeability and saturation is affected by the residual saturation and pore-size distribution of the porous medium. For isotropic media, the relative permeability of the wetting phase (during the drainage cycle) and the non-wetting phase can be approximated by the Burdine equations, (Laliberte [25]).

$$k_{rw} = \left(\frac{S-S_r}{1-S_r}\right)^2 \frac{\int_o^S \frac{dS}{P_c^2}}{\int_o^1 \frac{dS}{P_c^2}} \tag{2.14}$$

and

$$k_{rnw} = \left[1 - \left(\frac{S-S_r}{S_c-S_r}\right)\right]^2 \frac{\int_S^1 \frac{dS}{P_c^2}}{\int_o^1 \frac{dS}{P_c^2}} \tag{2.15}$$

where

S_c = critical saturation, (saturation at which the non-wetting phase becomes discontinuous and which corresponds approximately to the saturation at the bubbling pressure, P_b).

Corey (noted by Laliberte [25]) found experimentally that for relatively homogeneous and isotropic media having an average pore-size distribution ($\lambda = 2$ approx.), equations (2.14) and (2.15) could be approximated by

$$k_{rw} = S_e^4 \tag{2.16}$$

and

$$k_{rnw} = (1 - S_e)^2(1 - S_e^2) \quad . \tag{2.17}$$

Laliberte [25] shows that "ε" in the more general equation,

$$k_{rw} = S_e^{\varepsilon} \tag{2.18}$$

could be approximated by the relation

$$\varepsilon = \frac{2 + 3\lambda}{\lambda} \quad . \tag{2.19}$$

Porous media of completely uniform pore-size distribution have an exponent $\varepsilon = 3.0$ and for unconsolidated sands having a single grain structure, $\varepsilon = 3.5$.

Dealing with air-water-snow systems, Colbeck [10] mentions the use of $\varepsilon = 3$ in the relative permeability-effective saturation relationship (eqn.2.18). However, he uses $\varepsilon = 2$. In later publications [13], [15], [16], Colbeck uses $\varepsilon = 3$. Friesen [22] obtained $\varepsilon = 3.3$ and $\varepsilon = 3.2$ for snow densities of 0.40 gm/cm^3 and 0.48 gm/cm^3 in the snow-soltrol C systems.

C. WATER FLOW THROUGH SNOW

An understanding of the water flow mechanisms in snow is of particular importance in the development of predictive capability regarding avalanche formation and the seasonal release of melt water. Knowledge of the mechanisms also finds application in the ice-capping process of snow roads. In recent years, general theories of fluid flow through porous media have been applied to the air-water-snow system and a theoretical basis for understanding the flow mechanisms has been developed. In this section, flow equations are reviewed and the results of pertinent studies are summarized.

General Flow Equations

Flow through porous media may often be considered from a macroscopic point of view and treated as irrotational flow. In addition, where the inertial forces are negligible as compared to the viscous forces during flow through an isotropic medium, Darcy's law may be applied. The general differential form of Darcy's equation is

$$q = -\frac{k}{\mu} \nabla P^* \tag{2.20}$$

where

q = volume flux, cm^3/cm^2-sec.,

k = permeability of the fluid, cm^2,

μ = dynamic viscosity of the fluid, $\frac{\text{dyne - sec}}{cm^2}$, and

P^* = piezometric potential, $dynes/cm^2$.

The piezometric potential, P^*, represents the resultant of the normal surface and body forces per unit volume acting on a volume element in a fluid of uniform density. P^* has the dimensions of energy per unit volume. If adsorptive forces are ignored, P^* becomes the summation of the pressure potential P, and gravitational potential ρgz. That is

$$P^* = P + \rho gz. \tag{2.21}$$

Equation (2.21) applies separately to the wetting and non-wetting phases.

For air-water systems where the air phase is at atmospheric pressure and static, equation (2.20) may be re-written as

$$q_w = - \frac{k_w}{\mu_w} \nabla(P_w + \rho_w gz) \tag{2.22}$$

where

q_w = volume flux of water, cm^3/cm^2-sec ,

k_w = effective water permeability, cm^2 ,

μ_w = dynamic viscosity of water, $\frac{\text{dyne - sec}}{cm^2}$,

P_w = water pressure, $dynes/cm^2$,

ρ_w = water density, gm/cm^3 ,

g = gravitational constant, cm/sec^2, and

z = relative vertical position, positive upwards, cm .

The associated continuity equation (water is assumed to be incompressible) is:

$$\text{div } q_w = - \phi \frac{\partial S_w}{\partial t} \tag{2.23}$$

where

ϕ = porosity, dimensionless,

S_w = water saturation, dimensionless, and

t = time, sec.

Combining equations (2.22) and (2.23) gives

$$\operatorname{div}\left[\frac{k_w}{\mu_w}\nabla(P_w + \rho_w g z)\right] = \phi\frac{\partial S_w}{\partial t} \quad . \tag{2.24}$$

Equation (2.24) is known as the Richards equation (Laliberte [25]).

Capillary pressure, as defined earlier, is the pressure difference across the interface of the two immiscible fluids. For the air-water system

$$P_c = P_a - P_w \tag{2.25}$$

where

P_c = capillary pressure, dynes/cm^2, and

P_a, P_w = pressure of the air and water phases respectively dynes/cm^2, (P_a = constant = 0 gauge pressure).

Combining equations (2.24) and (2.25) gives

$$\operatorname{div}\left[\frac{k_w}{\mu_w}\nabla(P_c - \rho_w g z)\right] = -\phi\frac{\partial S_w}{\partial t} \tag{2.26}$$

For one dimensional vertical flow, equation (2.26) becomes

$$\frac{\partial S_w}{\partial t} = -\frac{1}{\phi\mu_w}\frac{\partial}{\partial z}\left[k_w\left(\frac{\partial P_c}{\partial z} - \rho_w g\right)\right] \tag{2.27}$$

The Darcy and continuity equations for the air phase are similar to equation (2.22) and (2.23).

Capillary-pressure, Saturation Relationships

As an approximation to the snow-water system, Colbeck [13] performed capillary-pressure experiments (for the drainage cycle) with snow and kerosene at a temperature of - 10°C. A fine-grained snow (approximately 1 mm dia.) compacted to a density of 0.56 gm/cm^3, was used. The plotted results are shown in Figure 2.1 from which several observations may be made .

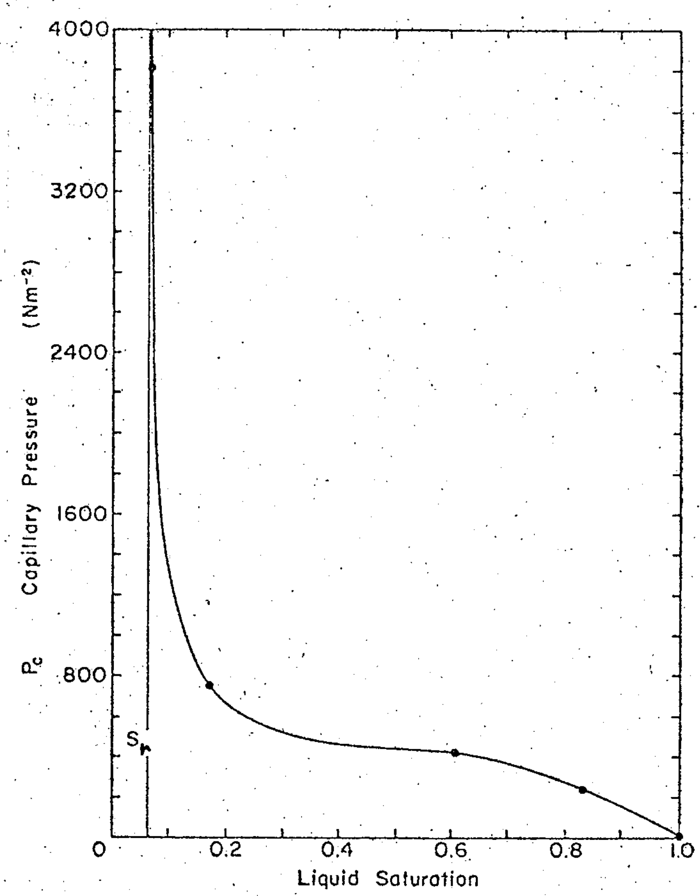

Figure 2.1 - Capillary pressure as a function of liquid saturation (after Colbeck, S.C. [13], The capillary effects on water percolation in homogeneous snow, Journal of Glaciology, Vol. 13).

The curve indicates a rapid desaturation which is typical of materials with a uniform pore size. Another important feature is the value of residual saturation $S_r \approx 0.07$. Since usually a narrow range of pore size occurs in snow, the relationship described in Figure 2.1 may be a good estimate for most types of snow. Colbeck [13] indicates however, that only a small part of the curve is significant with regard to water drainage in homogeneous snow since water saturations generally exist in the narrow range, $S = 0.1$ to $S = 0.2$.

Friesen [22] performed capillary pressure experiments with snow and soltrol C at a temperature of -15°C. Residual saturations of $S_r = 0.035$ and $S_r = 0.094$ were obtained for snow densities of 0.40 gm/cm^3 and 0.48 gm/cm^3, respectively.

D. HEAT AND MASS TRANSFER

There are three modes by which heat is transfered from one point to another: conduction, convection, and radiation. Because of the low temperatures associated with snow, the radiant heat component is usually negligible (Yen [44]). Also, according to Yen [44], thermal conductivity through interstitial air is often insignificant. Therefore, conduction through the ice skeleton, convection, and heat transfer due to vapour diffusion are the significant contributors to the overall heat flow. In dry snow a net mass transfer and redistribution of density occurs (constructive metamorphism) owing to the processes of sublimation, diffusion and condensation of the water vapour along the temperature gradient.

The general Fourier heat conduction equation for a medium containing no heat sources or sinks (no sublimation, vapour transfer, condensation, etc.) is:

$$\frac{\partial T}{\partial t} = \alpha \nabla^2 T \qquad (2.28)$$

where

T = temperature, °C,

t = time, sec ,

α = $K/\rho C_p$: thermal diffusivity, cm^2/sec ,

K = thermal conductivity, cal/cm-sec-°C,

ρ = density, gm/cm^3, and

C_p = specific heat, cal/gm-°C.

For one-dimensional heat conduction, equation (2.28) reduces to:

$$\frac{\partial T}{\partial t} = \propto \frac{\partial^2 T}{\partial z^2} \quad . \tag{2.29}$$

The heat transfer rate in the z direction for a particular time t, or for the steady-state condition, is described by the Fourier rate equation;

$$q_z = - K \frac{dT}{dz} \tag{2.30}$$

where

q_z = heat flux in the z direction, cal/cm^2-sec ,

$\frac{dT}{dz}$ = temperature gradient in the z direction, °C/cm, and

K = thermal conductivity, cal/cm-sec-°C.

Sulakvelidze (noted by Yen [44]) formulated a heat-transfer equation to account for the evaporation and condensation occurring porous media containing vapour; water or ice at temperatures close to the transition temperatures. This was done by including an additional term in the Fourier heat conduction equation. For one-dimensional heat transfer, Sulakvelidze's equation is:

$$\frac{\partial T}{\partial t} = \propto \frac{\partial^2 T}{\partial z^2} - \frac{L_s}{c_i \rho_s} q \tag{2.31}$$

where

$q = \frac{\partial C}{\partial t} - D \frac{\partial^2 C}{\partial_z^{\ 2}}$: the intensity of evaporation or condensation, gm/cm^3-sec ,

C = vapour concentration, gm/cm^3,

L_s = latent heat of sublimation, cal/gm,

c_i = specific heat of ice or snow, cal/gm-°C ,

ρ_s = density of snow, gm/cm^3, and

D = mass diffusivity, cm^2/sec.

In dealing with snow-air systems, the concept of effective thermal conductivity has been applied extensively. Effective thermal conductivity (designated K_e) represents the net effect (excluding radiant transfer) of all the mechanisms acting in the heat flow. A general expression defining K_e is:

$$q = K_e \text{ grad } T \tag{2.32}$$

where

q = heat flux, cal/cm^2-sec ,

K_e = effective thermal conductivity, cal/cm-sec-°C , and

T = temperature, °C.

Measurements of effective thermal conductivity have been obtained by several investigators. Where the results have been empirically correlated to structural properties, snow density was the sole parameter. Yen [44] summarized the results of several investigations shown in Table 2.1. (ρ_s = snow density, gm/cm^3).

TABLE 2.1

Effective Thermal Conductivity (K_e) of Dry Snow

Investigator	Empirical expression	Density range
Abels	$0.0068\rho_s^2$	$0.14 < \rho_s < 0.34$
Jansson	$0.00005 + 0.0019\rho_s + 0.006\rho_s^4$	$0.08 < \rho_s < 0.05$
Van Dusen	$0.00005 + 0.0010\rho_s + 0.0052\rho_s^3$	
DeVaux	$0.00007 + 0.007\rho_s^2$	$0.1 < \rho_s < 0.6$
Kondrat'eva	$0.0085\rho_s^2$	$0.35 < \rho_s$
Bracht	$0.0049\rho_s^2$	$0.19 < \rho_s < 0.35$
Sulakvelidze	$0.0012\rho_s$	$\rho_s < 0.35$
Proskuriakov	$0.000005 + 0.00242\rho_s$	

(after Yen, Y.C. [44], Recent studies on snow properties, Advances in Hydroscience, Academic Press, New York).

The significant heat transfer mechanisms in dense snow are conduction through the ice skeleton and the pore space. The effective thermal conductivity of dense snow is expressed by Schwerdtfeger (Yen [44]) as,

$$K_e = \frac{2K_s + K_a - 2\,\phi\,(K_s - K_a)}{2K_s + K_a + \phi\,(K_s - K_a)}\,K_s \tag{2.33}$$

where

K_e = effective thermal conductivity, cal/cm-sec-°C,

K_a, K_s = thermal conductivity of air and snow respectively, cal/cm-sec-°C,

ϕ = $1 - (\rho_s/\rho_i)$: porosity of snow, dimensionless, and

ρ_s, ρ_i = density of snow and ice respectively, gm/cm^3.

For a liquid saturated porous medium, Somerton (noted by Adam and Wilson [3]) proposed the expression

$$K_e = K_s\left(\frac{K_l}{K_s}\right)^{C\phi} \tag{2.34}$$

where

K_e = effective thermal conductivity, cal/cm-sec-°C,

K_s, K_l = thermal conductivity of the solid and liquid respectively, cal/cm-sec-°C,

ϕ = porosity of the solid matrix, dimensionless, and

C = empirically derived correction (≈ 1.0).

In the case of a flowing liquid phase, the heat transfer process is complicated by convection. Based on the comprehensive review by Adam and Wilson [3], the problem may be formulated by the heat balance equation:

$$\frac{\partial}{\partial z}\left[K \frac{\partial T}{\partial z}\right] - C_w \frac{\partial (vT)}{\partial z} = \frac{\partial (C_a T)}{\partial t} \tag{2.35}$$

where

K = thermal conductivity, cal/cm-sec-°C,

v = fluid flux, cm/sec ,

C_w = volumetric heat capacity of water, cal/cm^3-°C,

$C_a = C - L\rho_i \frac{\partial \theta_i}{\partial T}$: "apparent" volumetric heat capacity of the system, cal/cm^3-°C,

C = volumetric heat capacity, cal/cm^3-°C,

L = latent heat of fusion, cal/gm ,

ρ_i = ice density, gm/cm^3 , and

θ_i = volumetric ice content, cm^3/cm^3.

E. SNOW MECHANICS

Snow mechanics is a relatively new subject of scientific-technical research. Conventionally, the study of snow mechanics has been based on analogy to soil mechanics; however, difficulties arise due to the strong time and temperature dependence of many snow properties.

Bader [6] and Mellor [30] provide an extensive review of the mechanical properties of snow. Their review forms the basis of the following summary.

Densification

Undisturbed snow which has undergone destructive metamorphism (a few days following initial deposition) has a density usually above 0.15 gm/cm^3 and a grain size typically of about 1 mm. The structure of this low density dry snow can be conceptualized as a packing of granules with some of the grains removed. Thus there are relatively large pore spaces into which grains can move when the structure is deformed. Densification occurs due to shearing of the contact areas without deformation of the individual grains. At a density of around 0.5 gm/cm^3, the condition of close packing is approached and further densification is not possible without grain deformation. The rounded grains (due to destructive metamorphism) achieve relatively small contact areas and thus contribute to low strength. Constructive metamorphism further contributes to a decrease in strength of the lower layers.

By reconstituting snow (mechanically disaggregating, milling, mixing, etc), a density increase accompanied by a significant increase in strength is achieved. The increase in strength is due to the growth in contact area promoted by the more intimate contact of fractured grains of different temperatures.

Response to Rapid Loading

A well bonded, dense snow behaves as a compressible viscoelastic material. That is, for a very short time interval it can respond elastically under moderate load, with strains which are proportional to stress and which are recoverable on removal of the load. With sustained loads, however, deformation is largely viscoplastic and is irrecoverable. The relationship between Young's modulus and density (Greenland snow) was investigated by Bentley, Lee and Nakaya (Mellor [30]) and is shown in Figure 2.2.

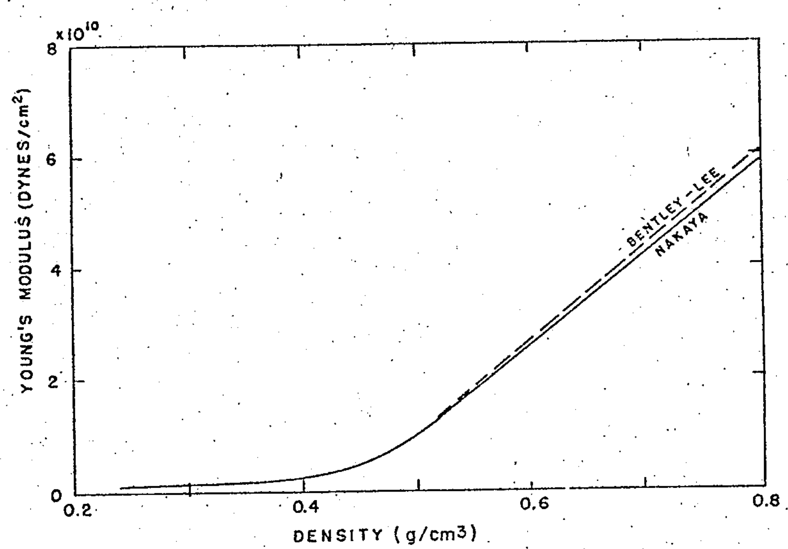

Figure 2.2 - Relationship between dynamic Young's modulus and snow density for a range of Greenland snow types at -9°C. (After Mellor [30], Polar snow - A summary of Engineering Properties, MIT Press, 1963).

For the naturally compacted snows of Figure 2.2, Young's modulus (E) follows the relationship

$$E = 6.3 \times 10^{6} \exp 14.6\rho \quad \text{dyne/cm}^2, \tag{2.36}$$

for the density range $0.27 < \rho < 0.5$ gm/cm^3, and

$$E = (16.4\rho - 7.20) \times 10^{10} \quad \text{dyne/cm}^2, \tag{2.37}$$

for the density range $0.5 < \rho < 0.9$ gm/cm^3. It was also found that for a given density, E tended to increase with a decrease in temperature and decrease with grain size. The inability at present, to assign numerical values to textural characteristics makes rigorous definition of relationships difficult.

The investigations in Greenland by Bentley, Pomeroy and Dorman (Mellor [30]) have shown that Poisson's ratio varies very little with changes in density. For snow with density between 0.4 and 0.7 gm/cm^3, Poisson's ratio is given by:

$$\nu = 0.15\rho + 0.2 \tag{2.38}$$

where

ν = Poisson's ratio, cm/cm, and

ρ = snow density, gm/cm^3.

The tests performed by Lee on high-density processed snow (noted by Mellor [30]) are in agreement with equation (2.38).

Butkovich, Ramseier and Gow carried out extensive investigation into the strength of snow. The relationships between strength and density, as summarized by Bader [6] and Mellor [30], are shown in Figures 2.3, 2.4 and 2.5.

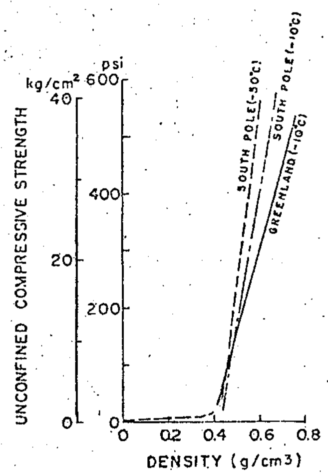

Figure 2.3 - Unconfined compressive strength versus density for naturally compacted snow from Greenland, and the South Pole. (Temperature - 10°C)

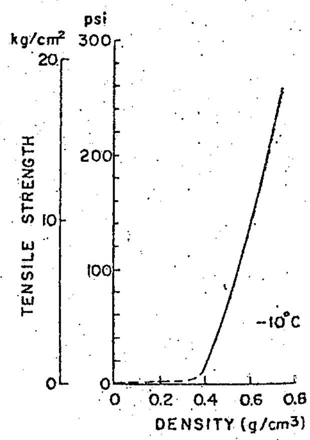

Figure 2.4 - Tensile strength of high density snow at a temperature of -10°C (-10°C has been adopted by the U.S. Army Cold Regions Research and Engineering Laboratory as the standard test temperature).

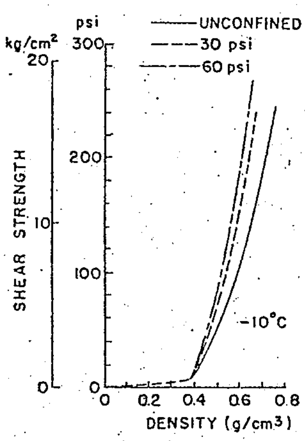

Figure 2.5 - Strength in double shear plotted against density for the unconfined case and for normal pressures of 30 and 60 psi. (Temperature - 10°C).

Many attempts have been made to apply the Coulomb equation to snow. The Coulomb equation, as applied in soil mechanics relates shear strength with normal pressure in the linear form;

$$s = c + p \tan \phi \tag{2.39}$$

where

s = shear strength, psi,

p = normal pressure, psi,

c = coefficient of cohesion, psi, and

ϕ = angle of shearing resistance.

In the case of snow, the plot of shear strength against normal pressure is not linear. However, in studies of oversnow vehicles (Diamond [19], Nuttall, Thomson [34], et al) where normal pressures lie in a narrow range (0 to 10 psi), the portion of the curve is often approximated with a straight line. In this connection, studies made over a wide range of surface snow densities and temperatures indicate variations in 'c' ranging from 0 to 1.6 psi and values of 'ϕ' ranging from 21° to 55°.

Response to Sustained Loading

In most construction materials, a detectable rate of creep is often considered to be a failure. In snow, where relatively high creep rates in engineering practice are tolerable, failure is identified with collapse rather than with creep.

The strain rate due to sustained loading does not bear a linear dependence on stress but rather exhibits an exponential type of relationship. It has been found that the creep rate of snow can be represented by the hyperbolic sine function;

$$\dot{\varepsilon} = A \sinh \frac{\sigma}{\sigma_o} \tag{2.40}$$

where

$\dot{\varepsilon}$ = strain rate, sec^{-1},

σ = stress, gm/cm^2, (where stress is expressed in mass units, the force associated with the mass is implied),

σ_o = a constant having the stress units, and

A = A value dependent on the snow density.

The creep rate is highly dependent on density and the value of 'A' in equation (2.40) varies as the snow is strained. Bader [6] indicates that when stresses are always above 800 gm/cm^2, equation (2.40) may be simplified to

$$\dot{\varepsilon} = \sigma_o \sinh \frac{\sigma}{\sigma_o} . \qquad (2.41)$$

At a 10% error limit, equation (2.41) may be further simplified to

$$\dot{\varepsilon} = \frac{\sigma_o}{2} \exp \frac{\sigma}{\sigma_o} \qquad (2.42)$$

where

σ_0 = 700 gm/cm^2.

Where stresses do not exceed 600 gm/cm^2, a direct proportionality between stress and strain rate may be assumed.

Creep rate can also be expressed as an exponential of the density by the relationship;

$$\dot{\varepsilon}_1 = \dot{\varepsilon}_0 \, e^{-b(\rho_1 - \rho_0)} \qquad (2.43)$$

where

$\dot{\varepsilon}_0$ = strain rate at time t = 0, sec^{-1}

$\dot{\varepsilon}_1$ = strain rate at some later time t = 1, sec^{-1},

ρ_o, ρ_1 = snow densities at t = 0 and t = 1 respectively, gm/cm^3, and b = a parameter which behaves nearly as a constant with a value of 21.05 most frequently found. It is believed that 'b' is dependent somewhat on snow type, time sequences and temperature.

The range of creep rate within which the relationship of equation (2.43) is valid is not known. Bader [6] indicates that the theory of equations (2.40) and (2.43) for which $\sigma_0 = 700\ gm/cm^2$ and $b = 21.05$, fails at stresses (σ) that are greater than 5 kg/cm^2 and at densities (ρ) greater than 0.84 gm/cm^3. It is interesting to note that at these densities a permeable snow no longer exists but rather a porous ice.

F. INDEX PROPERTIES

Field identification and classification of snow type for any given purpose is not a well-developed subject. Although no standard for field investigation exists, review of published material suggests a consensus that at least the determination of density, grain size, grain shape, temperature and hardness be the minimum criterion. These properties will be referred to henceforward, as the index properties of snow.

Density

The density (mass per unit volume, gm/cm^3) is perhaps the most significant index property of snow. The average density is usually determined by simply weighing a known volume of snow, or melting a known volume of snow and measuring the volume of melt water. Stainless steel tubes are generally used to obtain the snow sample. More sophisticated techniques such as radiation scanning and attenuation measurement are used in more precise laboratory work. Bader [2] notes that for the purpose of correlation with other properties, the determination of snow density to two significant figures is often insufficient.

Grain Size

With reference to grain size, snow is usually described qualitatively as being either fine, medium, coarse, or very coarse-grained. A system of classification, presented below in Table 2.2, was proposed by Schaefer, Klein, and deQuervain. The predominating grain diameter is determined by direct inspection with the aid of a hand lens and plate having a 1-mm grid.

TABLE 2.2

Snow Classification

Predominating grain diameter (mm)	Designation	
< 0.5	very fine grained	(vfg)
0.5 to 1.0	fine grained	(fg)
1.0 to 2.0	medium grained	(mg)
> 2.0 to 4.0	coarse grained	(cg)
4.0	very coarse grained	(vcg)

(after Bader [6], The physics and mechanics of snow as a material, CRREL Research Report, 1962)

Depending on the nature of the investigation, grain size may be measured under a microscope or by screening or elutriation. When snow is screened into fractions, Bader [6] proposes the following definition of mean grain diameter.

$$d = \sqrt{Mm} \tag{2.44}$$

where

d = mean grain diameter of a fraction, mm ,

M = side length of square mesh openings through which the fraction passes, mm , and

m = side length of square mesh openings on which the fraction is retained, mm.

The mean grain diameter of the mixture is:

$$d_s = \frac{\sum_{i=1}^{n} (W_i d_i)}{\sum_{i=1}^{n} (W_i)} \tag{2.45}$$

where

d_s = mean grain diameter of the mixture, mm.,

n = number of fractions,

d_i = mean grain diameter of i^{th} fraction, mm , and

W_i = weight of i^{th} fraction, gm/cm^3.

Grain Shape

A large variety of grain shapes occur in freshly deposited snow. The reason being that the snow flake shape depends on the atmospheric conditions in which the ice crystals grow. New snow is commonly classified; stellar, column, plate, needle, capped column, or spacial dendrite, depending on the geometric features of the snow flakes. These distinct features, however, soon disappear following the initial deposition.

Grain shape is observed generally to determine the stage of metamorphism (identification of depth hoar, etc.) and for deciding whether a given dry snow has or has not been previously wet.

Temperature

In the classification of materials, temperature is not usually considered to be an index property. However, since so many properties of snow are highly temperature dependent, temperature must be specified. Snow can exist at temperatures $\leq 0°C$.

Hardness

Evaluation of the strength parameters by direct means is usually laborious and time-consuming, and hence of limited utility in the field. Attempts have been made to devise indirect methods which provide a quantitative correlation to the funadmental strength parameters. These indirect methods are generally based on some form of penetration test.

Perhaps the most popular of the field testing procedures is the determination of a hardness number by means of the Rammsonde cone penetrometer. The measure of "hardness" (kg) is based on the penetration of a cone under an impact of known energy (discussed in Appendix C). The Rammsonde instrument is used in the study of undisturbed snow covers as well as the compacted snow surfaces of snow roads and runways.

The Rammsonde (Ram) hardness necessary for supporting various wheel loads and tire pressures for a specified number of wheel coverages (Figure 2.6) has been determined by Wuori [43]. The hardness values represent the lowest hardness permissible in the top 15 cm of the prepared snow surface. An additional requirement is that the underlying layers have a hardness of at least 75% of the surface layer.

The Rammsonde hardness of a snow pavement has also been correlated to the unconfined compressive strength. Clark, Abele, and Wuori [9] present a nomograph (Figure 2.7) in which the unconfined compressive strength is related to various wheel loads, contact pressures and number of wheel coverages. The use of the

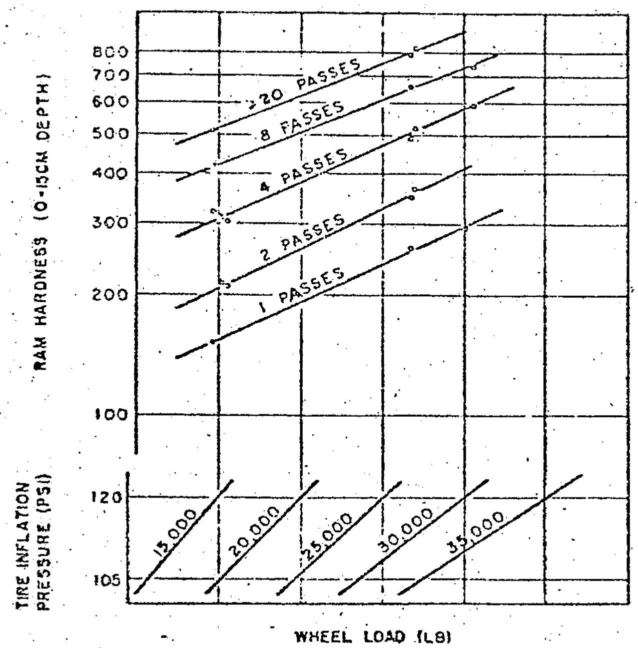

Figure 2.6: Required ram hardness for supporting various wheel loads. The abcissa indicates wheel loads at various tire inflation pressures. (after Wuori [43], Supporting capacity of processed snow runways, CCRREL, 1962)

Rammsonde penetrometer in conjunction with a prepared nomograph, as shown in Figure 2.7, facilitates quality control during construction of snow pavements as well as the monitoring of performance during operation.

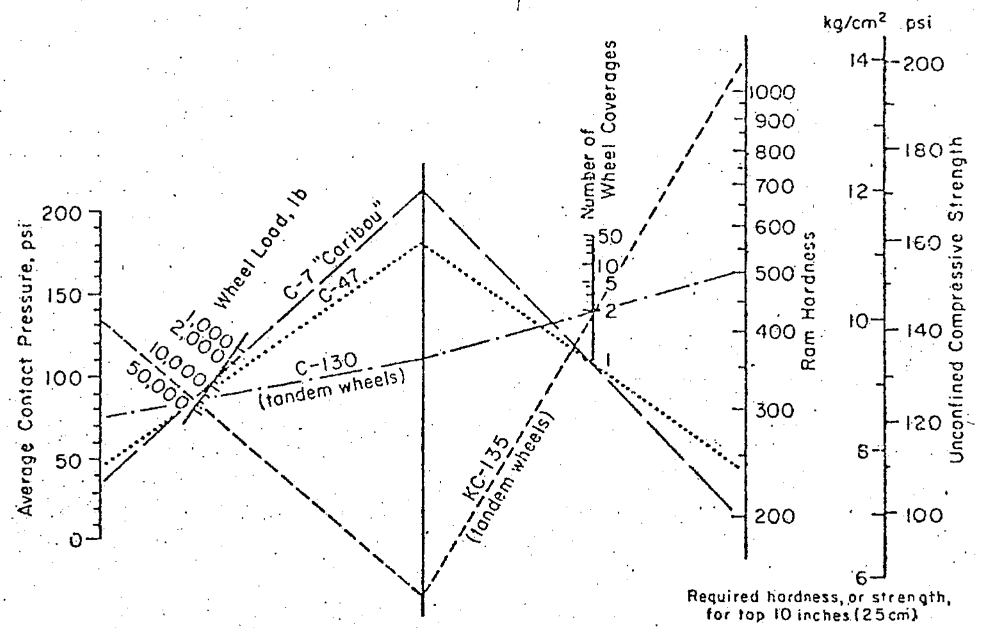

Figure 2.7: Required hardness (or strength) of a snow pavement for various wheel load conditions. Examples in the use of the nomograph are shown for various aircraft. (after Clark, Abele, and Wuori [9], Expedient snow airstrip construction technique, CRREL, 1973)

In Figure 2.8, deQuervain (noted by Martinelli [29]), illustrates a good correlation between ram resistance (hardness) and the tensile strength of new snow. The results indicate age hardening, and show the tensile strength for snow four (4) days old or older to be $\approx$ 1.5 times greater than the tensile strength of younger snow with the same ram resistance. Age hardening in snow is highly temperature dependent, however no reference to temperature history is made.

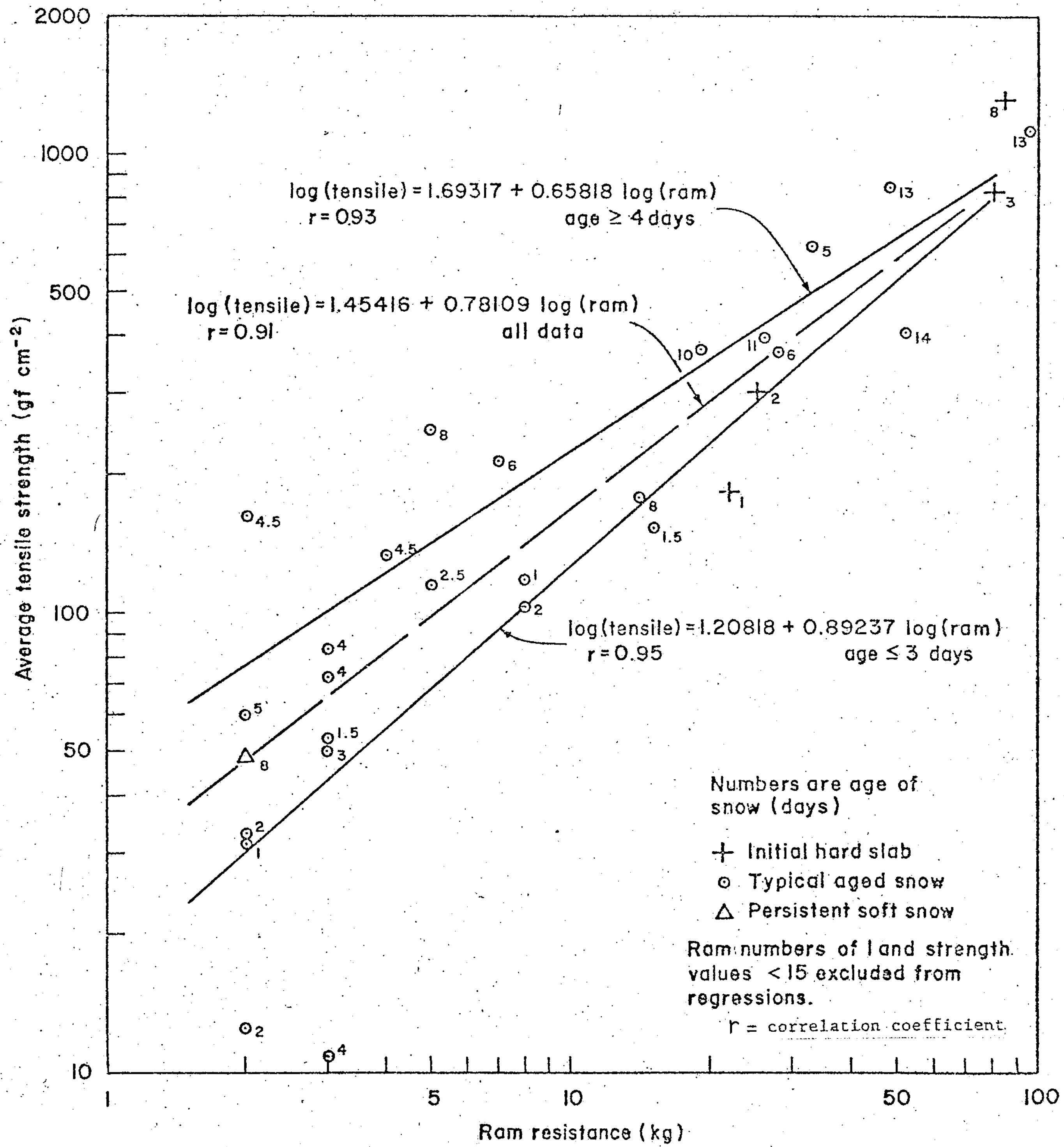

Figure 2.8: Average tensile strength as a function of ram resistance and age (after deQuervain, Martinelli [29], Physical properties of alpine snow as related to weather and avalanche conditions, U.S. Department of Agriculture, Forest Service, 1971)

A number of investigators have correlated Rammsonde hardness to snow density. Martinelli [29] summarized the regression and correlation coefficients for several sets of data fitted to the regression

$$\log R = a + b\rho \tag{2.46}$$

in Table 2.3 where

R = rammsonde hardness number, kg, and

ρ = snow density, kg/m^3.

TABLE 2.3

Summary of Regression and Correlation Coefficients

Source	a	b	Correlation coefficient (r)	Age of snow	Density range
					kg m^{-3}
Bull (1956)	−0.6107	0.00531	0.80		
Keeler & Weeks (1967)	− .8446	.00640	.94	<4 months	100 − 510
Keeler (1968)	− .7482	.00599	.89	<4 months	150 − 430
1	− .428	.00543	.84	$\leq$14 days	40 − 450
2	− .305	.00343	.54	$\leq$1 month	100 − 390
3	− .463	.00421	.68	$\leq$4 months	100 − 430

(after Martinelli [29], Physical properties of alpine snow as related to weather and avalanch conditions, U.S. Department of Agriculture, Forest Service, 1971)

Polar snow of Greenland was studied by Bull (1956) and dry seasonal snows of Montana by Keeler and Weeks (1967, 1968). Alpine snow (source 1) and snow from a sheltered opening near source 1 (source 2, 3), were studied by Martinelli. No reference to temperature is made in these studies.

Ager [4] studied the influence of temperature on the density and hardness of snow in the temperature range from -1°C to - 23°C . He found that for a given compactive effort, highest densities were achieved at - 1°C. Subsequently, highest hardness values were obtained when the compacted sample was cooled to - 23°C. He also found that the density and hardness was much more sensitive to temperature variation in fine-grained snow than in coarse-grained snow.

The studies of Abele, Wuori, Clark, et. al., suggest that correlation of snow hardness to temperature (at particular density) is perhaps a more meaningful approach to the density, hardness, temperature interrelationship of snow.

CHAPTER III

WINTER ROADS

The idea of compacting snow as a means of improving oversnow trafficability, is extremely old. The snow road of the horse and sled age was compacted by primitive means - today, accomodation of heavy-wheeled traffic necessitates improved methods in the construction of snow pavements.

Many studies directed towards obtaining a better traffic foundation, have been carried out. The literature produced by a number of these investigations, is reviewed in Chapter III. Salient observations and conclusions are cited in order that a procedural guide, for the construction of snow pavements, may be developed.

System of Classification

To dispel any confusion regarding the terminology used in this study, a complete classification of winter roads is presented. The system of classification proposed by Adam [1], is adopted herein.

Winter Trail - "a trail used only in winter between freeze-up and break-up, and which is established by a single pass of a wheeled or tracked vehicle using a 'blade' if necessary to gain access."

Snow Road - "a road built primarily by using snow as cut and fill material to establish some resemblance to a constructed road grade. Compaction is part of the construction procedure. A snow road can be further classified by whether the snow is agitated or 'processed' before compaction:

i) Compacted Snow Road - the snow is compacted without 'processing'.

ii) Processed Snow Road - the snow is processed before compaction."

Ice Road - "a snow road with the physical addition of water to form a bonding agent between snow particles in order to give added stability to the roadway itself. Ice roads are similar to snow roads, in that they can be sub-classified as compacted or processed. (Ice roads should not be confused with winter roads on lake or river ice, which are sometimes erroneously referred to as ice roads)."

Winter Road - "this name applies to all three classifications; namely, winter trail, snow road and ice road. It is any road that carries traffic only over the winter period."

Ice Bridge - "an artificially thickened ice cover that provides the required weight capacity at river crossings or other bodies of water."

Route Selection

Although the discussion of route selection is a deviation from the main thrust of this study, the importance of the subject justifies a few brief comments. As pointed out by Adam [1,2], performance evaluation of winter roads must include trafficability aspects as well as environmental considerations. Trafficability can be improved, and operation and maintenance costs reduced, if shallow gradients and flat curvatures are maintained. Also, the degradation of underlying permafrost in permafrost areas, and drainage and erosion problems may be minimized or avoided through proper route selection.

Measures to Increase the Bearing Capacity of Snow

The successful construction of winter roads requires a knowledge of the basic mechanisms by which the strength of snow increases. To gain a qualitative perspective, the mechanisms are reviewed.

Studies by Ager, Clark, Abele, Wuori, et al, have shown that snow strength increases with an increase in density and a decrease in temperature. In addition, bond growth occurring between the individual snow grains (age hardening or sintering), makes a significant contribution to strength increase.

It has been found that by mechanically agitating (processing) the snow, a more non-uniform particle size distribution is produced. This allows (upon compaction) more intimate grain-to-grain contact which results in an increase in density and an acceleration of the age hardening process. The disaggregation and compaction of snow is most effective if performed at higher temperatures (below freezing), however after that, lower temperatures are desirable to achieve high strength.

The age-hardening of snow is highly temperature dependent. Hardening rates are higher at higher temperatures (below freezing), however snow which is age-hardened at a lower temperature will ultimately reach a higher strength.

A. SNOW ROAD CONSTRUCTION

Snow roads are basically constructed of compacted in-place snow or compacted processed snow. The available literature describing the construction experience is extensive, as is the variation in construction technique and construction equipment used. An outline of the basic steps in snow road construction is presented followed by a review (limited to a selective cross-section of the literature) of construction methods and results.

A thorough literature research (winter roads, environmental implications, etc.) and catalogue of abstracts is presented by Adam [1].

1. Initial Site Preparation

Following the first major snowfall of the season, an initial dragging operation is performed. A simple wooden drag is towed by a low-pressure tracked vehicle to promote frost penetration and to smooth out minor surface irregularities. When a sufficient snow cover has accumulated, and the underlying ground is sufficiently frozen, snow road construction may be started.

In permafrost regions (where this preparatory stage is especially applicable) caution must be exercised not to remove too much cover vegetation and thus cause degradation of the underlying permafrost in subsequent years.

2. Disaggregation/Processing

There is general agreement in the literature that compaction alone, on in-place snow, will not be sufficient to achieve the strength required of snow surfaces subjected to intensive wheeled traffic. That is, the effects of compaction alone are usually too limited in depth to provide a sufficiently thick snow pavement. Depth processing is therefore required and the types of equipment used for this purpose have been rotary earth tillers, versions of the farm harrow, rotary snow plows, and pulvimixers.

3. Leveling - Compacting

For maximum effectiveness, the compaction should be performed immediately after disaggregation, that is, before the processed snow has a chance to 'set-up' (age harden). Any leveling required is performed prior to or during the compaction.

The leveling is usually performed by towing a steel or wooden drag. The drag may be a simple frame-like apparatus fixed with cutting edges or a ballasted pontoon-type assembly. Depending on the weight and design, the drag may serve a dual purpose of leveling and compacting. Where major leveling of irregularities or shaping is required, backblading with a bulldozer is performed.

Compaction is usually performed by dragging and/or rolling with large diameter (8 or 10 ft) rollers. An additional compactive effort is provided by the tracks of the tow vehicle. Vibratory compaction equipment have also been studied, however, this type of equipment is not extensively used.

4. Preparing Final Surface

The final grading is usually performed using a finishing drag or snow plane, followed by a final rolling. The finishing drag or snow plane is fixed with adjustable cutting blades permitting a smoother surface to be achieved. This type of equipment is predominantly used in snow airstrip construction. If the roadway is sufficiently age hardened, the conventional road grader may be used to remove high spots and fill in depressions. An effort must be made to achieve as smooth a surface as possible during the initial compaction as the low spots filled by the grader, at this stage, generally remain weaker even after the final rolling.

Ice-capping of snow roads, as a means of achieving a road surface capable of withstanding a high intensity of heavy wheeled traffic, has been studied. The ice-capped snow road is a processed and compacted snowbed which has water applied to the surface to increase its density and strength. Methods of increasing road strength and surface durability, by heat application during disaggregation and surface finishing, have also been investigated.

B. CONSTRUCTION METHODS AND RESULTS

The Scandinavian Experience

Ager [5] discusses the snow compaction tests carried out in Lycksele (1956), by the Forestry Society and Royal Domain Administration (S.D.A.) of Sweden. Although the methods described are applicable only to horse and tracked vehicle roads, the tests identify the significance of snow processing in snow road construction. The results of the tests were compared to the results produced by the traditional method of snow road construction, where the snow is first processed throughout the roadbed, with a deeply penetrating track-type tractor, and then dragged.

The following equipment was used in the tests: a wooden drag (3 blades) having a contact pressure of 0.035 kg/cm^2, a rail-roller (open type) having an approximate weight of 450 kg per 1.5 m length, a closed roller which was constructed by covering the rail-roller with corrugated sheet metal, a pontoon drag 2 m long and weighing 180 kg, a rotary tiller, and an Oliver OC 3 tractor equipped with standard tracks.

The test results, for various combinations of the equipment, compared as follows. Roads constructed by a single snow processing, using the rail-roller, followed by a single compaction pass with the pontoon drag or the closed roller, were equivalent in quality to the roads constructed by the traditional method. A double processing with the rail-roller, followed by a single compaction with the pontoon drag or closed roller, produced roads with hardness (strength) values approximately 40% greater. A double processing with the rotary tiller, however, followed by a single compaction with the pontoon drag, yielded considerably higher bearing strength values.

Leijonhufvud [26] describes similar experience in the construction of snow roads intended for horse-drawn and tracked vehicle traffic. Agricultural equipment such as the spring harrow, the disc harrow and the rotary tiller were used to process the snow. The best processing results were achieved using a modified rotary tiller where the original rigid tines were replaced by chain flails. Leijonhufvud also points out the superior depth effect produced by roller compaction as compared to drag compaction. The drag, however, produces a harder snow surface due to the crushing and grinding of the snow particles in the surface layer.

The conditions necessary for hardening of a snow cover may vary depending on the type of snow and on the temperature. To achieve a desirable hardness in snow roads, a fine grained snow compacted to a high density is initially required. The fusion of snow particles (sintering), however, is dependent on the availability of free water or water vapour. Ager [5] carried out experiments on the hardening process of compacted snow during which he insulated the road bed either from the atmosphere or the ground surface or both. He found that a newly compacted snow road hardens from the bottom upward independently of the prevailing weather conditions, but the hardening of the surface layers depends largely on the low temperatures of the air and on the penetration of low temperatures deep into the snow. It has been found that hardening which starts from the bottom is faster on peat soils than on mineral soils (Putkisto [35]).

Putkisto [35] states that the direct effect of the relative humidity of the air on the hardening of snow is probably comparitively small. However, an exceptionally low relative humidity may cause intense sublimation of snow, softening the upper layers and restraining the hardening process. It is also pointed out that an accumulation of fresh snow on a snow road insulates the road bed from the cold atmosphere and softening from below will occur.

As indicated by Ager [5], Putkisto [35] and Eriksson [21], the afternoon is generally the most favourable time for compacting snow. During this time of day, the snow has a relatively high temperature and thus has sufficient water vapour between the snow particles. Also, during the night when the temperature drops, freezing will occur. Putkisto [35] considers the most favourable meterological conditions for snow road construction to occur immediately following the cessation of low-pressure periods. That is, the cool air currents and lack of precipitation of high-pressure periods are most desirable. Furthermore, the construction should proceed during early winter as the size of snow particles (as pointed out in Chapter II), is more advantageous as regards to disaggregation, compaction and hardening.

The next section deals with the North American experience where a much heavier variety of equipment is used to construct snow pavements capable of withstanding a high intensity of wheeled traffic. It will be noted that the basic construction techniques and variables remain the same.

The North American Experience

1. Camp Hale, Colorado

In 1950, the U.S. Bureau of Yards and Docks carried out a series of tests on depth processing and compacting of snow, at Camp Hale, Colorado (U.S. Navy Tech. Pub. [40]). During the test period, (late January, 1950, to mid-March, 1951), the snow depths and temperature data were as follows:

average snow depth	17 in;
maximum snow depth	30 in;
average temperature	17°F;
maximum temperature	64°F; and
minimum temperature	-28°F.

The following equipment was used:

1) 8-ft-diameter, 8-ft-wide, 4-ton, hollow-shell, fixed-face, corrugated-steel roller;
2) pontoon barge drag, weighted to 7 tons with bearing pressure of 0.88 psi;
3) Seaman's 6-ft-wide pulvimixer;
4) disc harrow; and
5) 250,000-Btu/hr gasoline heater with a bearing pressure of 0.2 psi.

Based on the snow road densities obtained, the various techniques tried, rank in the following order.

1. Drag, pulvimixer, roller
2. Roller, disc harrow, drag
3. Roller

4. Pulvimixer, roller
5. Roller
6. Pulvimixer, drag
7. Pulvimixer
8. Pulvimixer, heater
9. Drag harrow
10. Disc harrow

The test road sections constructed by methods 1. and 2. withstood only limited traffic of a 4-ton 6 x 6 Army wrecking truck. The other test sections were not traffic-tested.

The report concludes that a multiple-pass procedure is more effective than the single-pass for increasing the density and in most cases for increasing the hardness. The conclusions also state that the multiple-pass procedure beyond the third or fourth pass is impractical. It is inferred that double or triple passes of the equipment were performed on the 10 test sections referred to.

2. Point Barrow, Alaska

During the 1950-51 winter season, several test strips were built using various combinations of snow stabilization equipment at Point Barrow, Alaska. The U.S. Navy Technical Publication [40] gives account of the 4 most effective combinations tested. The equipment and methods used, and the results obtained from the 4 test roads are summarized.

Section I - The snow cover (average 18 in.) was processed by a Seaman's, 6-ft-wide pulvimixer and immediately followed by an 8-ft-diameter, 8-ft-wide, 4-ton, hollow-shell, fixed-face, corrugated steel roller. Five passes of this combination, at 2-hour intervals, was performed. The pulvimixer operated with ease, cutting about 12 in into the snow on each pass, and the roller, exhibiting a high diameter to weight ratio, rolled freely without plowing. Subsequent tests indicated that the density of the entire depth of snow increased uniformly with no stratification. Hardness values, however, are not given.

The road section, subjected to a traffic test, withstood 20 continuous trips with a Jeep and 10 with an empty GMC 2 1/2-ton, 6 x 6 cargo truck. The resulting minor surface deterioration was easily repaired by a single pass of a light fixed-screed steel drag. A low-bed trailer, with a gross weight of 26 tons was then towed over the roadway, by a Caterpiller Model-12 motor grader. This caused shallow tire depressions along the line of travel which could be removed quickly by a pass of the drag and roller.

Section II - The equipment combination used in this road section was the pulvimixer, immediately followed by a surface heater and sheepsfoot roller. As in Section I, 5 passes of the equipment combination were performed at 2-hour intervals. The test results showed a marked increase in the density of the entire snow cover over that obtained in Section I, with the greatest increase near the surface. When subjected to the traffic test, however, 10 trips with the Jeep and 10 with the empty GMC 2 1/2-ton, 6 x 6 truck necessitated a maintenance pass with the steel snow drag. A single pass over the section with the motor grader and loaded 26-ton-gross low-bed trailer caused very shallow tire marks on the road.

Firm conclusions regarding the benefits of using a surface heater were not possible with the data available. The study points out, however, that the method of surface heating used on Section II is very inefficient because of the large quantity of heat lost to the atmosphere. Also, the surface heater towing speed, being approximately 0.85 mph (other equipment, 1.5 mph), increases overall construction time.

Section III - The snow was processed with the pulvimixer, followed by a water carrier and the 8-ft roller. Five passes of the equipment combination were made at a 15-hr interval between passes. The water carrier moved at a speed of 1.0 mph, discharging water at the rate of 50 gal/lin ft (0.5 lb/sq ft), through a spray bar 8 ft long and 2 1/2 in. in diameter. To prevent adherence of wet snow to the roller, a 30-minute interval was allowed between water application and rolling. The surface density of the finished roadway was very high, however for the application rate used, the water penetration was not complete and the lower layers remained at a low density.

The study concluded that although the water application had some effect, the test section was not significantly better than the one built using only the pulvimixer and roller (Section I). It was also observed that in regions such as the Arctic plains, lack of adequate water supplies would make the water application technique infeasible. As regards to trafficability, high ambient temperatures prevented adequate traffic testing of Section III.

Section IV - The snow was processed with the pulvimixer followed immediately by a pontoon barge drag with a 6,300-lb load. Five passes of the equipment combination were performed at a 24-hour interval between passes. It was found that the density increased uniformly with each additional pass, although the actual values are not given.

Due to high ambient temperatures the traffic tests were inconclusive. The study pointed out, however, that the pontoon barge drag was not satisfactory as a piece of snow stabilization or maintenance equipment because of its bulk and lack of maneuverability.

The Point Barrow Studies concluded; "a combination of agitation and rolling appears to be the most practical and effective means of stabilizing a snow road on the Arctic coastal plain". Furthermore, ..."the best method of maintaining a snow road is with a weighted steel or wood frame drag. Either drag followed by the 8-ft roller is very effective in restoring the surface to good condition".

3. Churchill, Manitoba

In 1951, a 12-mile section of snow road, 45 miles from Churchill, Manitoba and 2 miles from the shore of Hudson Bay was constructed and maintained by the Royal Canadian Engineers (U.S. Navy Tech. Pub. [40]). In this region, high winds are common, and the snow conditions are described to be analogous to those occurring on flat, exposed Arctic coasts. The temperatures during the test period (Mid-February to early April), ranged from -30°F to 15°F although higher temperatures of 20°F and 30°F were experienced in April. The equipment used, consisted primarily of; 1 ski-mounted Seaman's pulvimixer equipped with a chain flail consisting of 120 chains (5/8 in. diam.), each 15 in. in length; 3 variable-weight (3,175 lb to 5,800 lb by 75 lb increments), corrugated-steel rollers, 6-ft in diameter and 8-ft in width; and 5 tracked tractors.

The snow road, with a 15-ft surface width, was constructed by an initial buildup process, followed by the pulvimixer treatment and roller. Two tractors, initially spaced 45 ft apart, on opposite sides of the right-of-way, windrowed the snow in towards the center-line. The crests of the 2 final windrows, after 3 passes of each tractor, were 10 to 13 ft apart. The contraction in snow volume at this stage, starting with a snow density of 0.3 gm/cm^3 (18.7 lb/ft^3), was in the order of 40 or 50 percent. A rough leveling was then performed with the tracked tractors, followed by 5 passes, at 1-hour intervals, of the pulvimixer-roller combination. No satisfactory answer was obtained regarding the optimum number of passes of the equipment combination; however, it was concluded that the time interval between passes should be kept to a minimum and in no case should be allowed to exceed 2 hours. The build-up process was accomplished at the rate of 7 miles per day; however, the progress on the finished road depended on the single pulvimixer, limiting the construction rate to 3 miles per 24-hour working day, under favourable conditions. Favourable conditions are defined as terrain open and flat, snow depth under 3 ft , wind chill factor less than 2,100, and visibility at least half a mile.

The densities achieved ranged between 0.4 gm/cm^3 and 0.5 gm/cm^3 and upon completion of a road section, a 36-hour curing period was allowed before the road was subjected to traffic. The traffic consisted of: 3-ton trucks loaded to a gross weight of 9 tons, developing axle loads of 11,500 lb; 20-ton loaded sleds (moving at 25 mph) and tracked tractors. The actual traffic volume is not given in reference [40]; however, it is inferred that the traffic was more or less continuous over the test period. No failures occurred over any part of the road, and no evidence of deterioration of the road surface was visible at temperatures up to 20°F. The study concludes that the effect of the heavy traffic was to improve the bearing qualities of the snow pavement over the duration of the traffic testing.

4. Greenland

The basic technique of snow stabilization consists of depth processing followed by compressive compaction. In 1953, trials on variations of the basic technique were conducted by the U.S. Navy on the Greenland Ice Cap. The variations included double-depth processing and layer compaction. The construction of a snow-compacted runway during these trials, is described by Moser [31] and summarized below.

a. Precompaction Preparations - It was found that considerable grading of the wind-driven undulating snow surface (sastrugi) was necessary to produce a level surface for compaction. As a result, a ski-mounted snow plane for grading and leveling snow was developed. This 6,120-lb snow plane is mounted on 4 skis giving a bearing pressure of 2.5 psi, and is equipped with a 12-ft-wide combination planer bowl and grader blade. Approximately 12 to 24 hours after initial rolling with a 10,240-lb, 8-ft-diameter, 8-ft-wide steel roller, the area was leveled with the snow plane. Two independent rolling passes were performed during the initial rolling (1 to 4 hours between passes) and 2 to 3 passes of the plane were required to achieve a smooth and level surface. Allowing 24 to 48 hours of age-hardening after the levelling operation, the entire surface was double-rolled. Approximately 2 days later, the first depth processing was performed on the prepared snowbed.

b. Depth Processing - Depth processing of the prepared snowbed was performed using the Navy Model 42 snow mixer. The snow mixer is a modified engine-driven earth pulverizer, 8 ft wide, with a 42-in rotor. The modifications permitted an increase in the rotor peripheral speed from 2,480 to 5,665 fpm, and included a balanced ski mounting eliminating porpoising and providing initial compaction to the processed snow. At an average air temperature of 0°F, 3 mixing passes (at a 32-in depth of cut) were performed at 1-hour intervals, immediately followed by 3 roller passes. The snow particles ranged in size from 1 to 5 mm after one depth processing (3 mixer passes) and regardless of the number of additional mixer passes, further pulverizing was limited. The 3-pass mixing followed by 3-pass rolling produced a 16-in thick snow-mat that was 46% more dense than the natural snow (0.33 to 0.47 gm/cm^3) and within 3 days was 6 times as hard (39 to 231 R*). It was concluded that the number of mixer passes is dependent on the type of snow being processed and that old, perennial snow, such as that found in Greenland and Antarctica, requires three passes of the snow mixer for good pulverization and blending.

* The quantity R is the snow hardness index obtained with the Rammsonde cone penetrometer. The penetrometer is discussed in detail in Appendix C.

c. Double Depth Processing - During the trials, it was reasoned that by reprocessing a well-bonded, once-processed snow, a more thorough pulverization and consequently a smaller snow particle size might be attained. A double depth processing (3 mixer passes followed by 3 roller passes) was then applied to the top 10 in of the once-processed snow. The reprocessing produced smaller individual particle sizes, mostly ranging from 1 to 2 mm, raising the average snow density to 0.54 gm/cm^3. After 30 days of age hardening in an average air temperature of 14°F, the average hardness was raised to 635 R. Aircraft tests showed that the mat could generally support wheel loads up to 100 psi except for sporadic soft spots where the mat hardness was as low as 300R. The occurrence of soft spots resulted from poor quality control during the depth processing.

The hardness growth due to depth processing is illustrated in Figure 3.1.

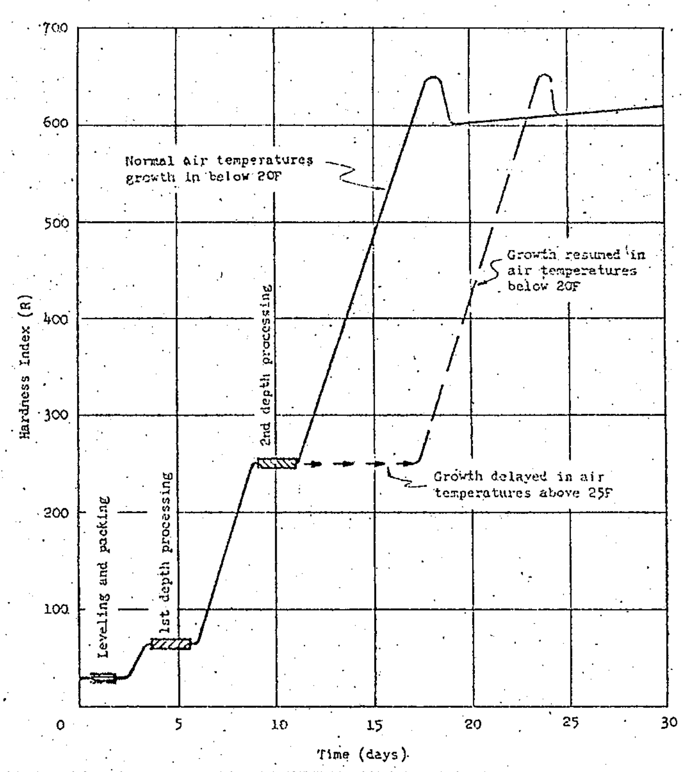

Figure 3.1 - Normal hardness growth in a single layer of polar snow. (After Moser [31], Navy cold-processing snow-compaction techniques, MIT Press, 1963.)

d. Surface Hardening - Rammsonde hardness tests performed on the double-depth processed snow mat, indicated that the hardness was not uniform with depth. That is, the bulk of the hardness occurred in the middle two-thirds of the mat. To improve the finish and hardness of the upper layer, a standard commercial 13-ton pneumatic-tired, 13-wheel roller was used followed by a 2,830-lb finishing drag. The finishing drag was constructed with cylindrical bottom skids and measured 20 in high, 7 1/2 ft long and 12 ft wide. A typical hardness distribution, occurring before and after surface hardening, is shown in Figure 3.2.

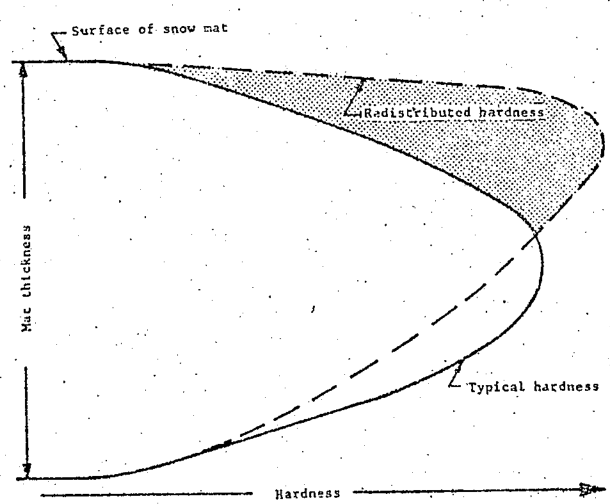

Figure 3.2 Typical vertical hardness in compacted snow compared with its redistribution after surface hardening. (after Moser [31], Navy cold-processing snow-compaction techniques, MIT Press, 1963.)

e. Layered Compaction - Two heavy layers of drift were deposited during the operation of the snow runway. The layers of drift were double-depth processed and a final mat consisting of the original 16-in layer plus a 9-in layer and an 8-in layer was produced. After testing with aircraft with various wheel inflation pressures, a tentative minimum hardness guide for compacted runways on deep snow was developed. The guide is shown in Figure 3.3.

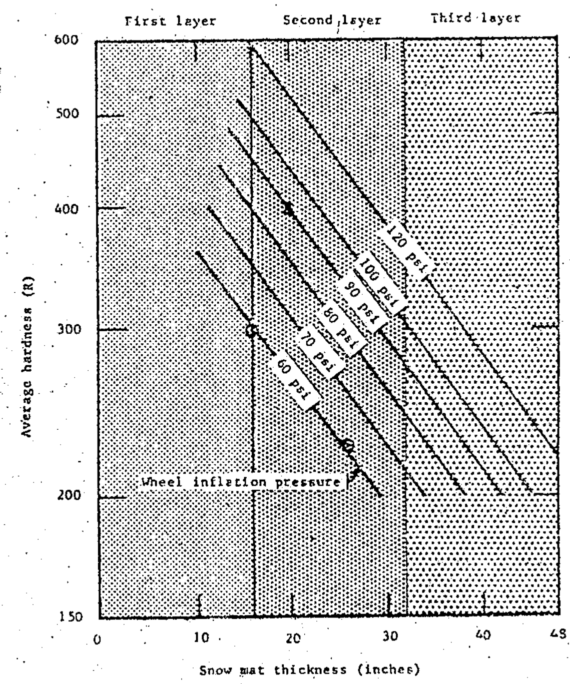

Figure 3.3 - Tentative minimum hardness guide for compacted-snow runways on deep snow. (after Moser [31], Navy cold-processing snow-compaction techniques, MIT Press, 1963.)

The layered compaction technique offered several advantages. Firstly, the runway was elevated above the natural snow surface, eliminating any fruther drift problems. Secondly, a more uniform load-bearing surface was achieved as the probability of coincidence of low-strength areas in the individual layers was very small. A logical conclusion is that the layered compaction technique allows a relaxation in the degree of control that is required to produce a uniform hardness in a single layer of snow pavement. However, the method generally requires transportation of borrowed material which could be both costly and time consuming.

In the same publication, Moser cites other examples, where the cold-processing methods described, have been used successfully. These include the 125-acre parking lot and 1-mile snow road at Squaw Valley, California (1960 Winter Olympic Games) and the 3-mile snow road at McMurdo Station, Antarctica (1960). Further detail on the U.S. Navy cold-processing technique and equipment is given by Moser [32], U.S. Navy [39], Camm [8] and Easton [20].

5. Kapuskasing, Ontario (1952-53)

The report entitled U.S.-Canadian Joint Compaction Trials [38] provides a comprehensive summary of the cold-processing and dry heat-processing techniques experimented with at various Canadian and U.S. locations. The experience gained at Kapuskasing, Ontario is representative of the joint effort.

During the course of the trials at Kapuskasing, Ontario, the following combinations of equipment were investigated:

1. a lane processed from 1 to 10 times by a pulvimixer with or without heat;
2. a lane processed from 1 to 10 times by a pulvimixer with or without heat followed by a roller or combination of rollers processing the same lane from 1 to 10 times;
3. a lane processed from 1 to 10 times by a roller or combination of rollers followed at varying intervals of time (1 to 24 hours) by a pulvimixer with or without heat, processing the lane from 1 to 10 times and followed finally by a roller or combination of rollers processing the lane from 1 to 10 times;
4. a lane processed from 1 to 10 times by a roller or combination of rollers;
5. A lane processed from 1 to 10 times by a Woods Preparizer; and

6. a lane processed from 1 to 10 times by a Woods Preparizer followed by a roller or combination of rollers processing the lane from 1 to 10 times.

The basic equipment referred to is detailed as follows:

Rollers - Several rollers of different type and weight were used. The rollers used most extensively and successfully were: a segmented steel roller (4, 2-ft segments individually mounted), 10 ft in diameter and weighing 22,400 lbs; a 10-ft diameter corrugated roller 8 ft long and weighing 7,700 lbs ; a William Bros. rubber-tired roller weighted to a gross weight of 38,000 lbs giving a unit tire pressure of 110 psi.

Pulvimixers - Seaman's pulvimixers with maximum rotor operating speeds of 275 rpm were used. Two of the pulvimixers were modified by the attachment of heaters to the canopies. In this modification, 2 sizes of heaters were used - one heater capable of turning out approximately 1,000,000 Btu/hr and the other 5,000,000 Btu/hr.

Woods preparizer - The Woods preparizer is a standard pavement breaker with a mechanical action similar to that of the Seaman's pulvimixer. The Woods preparizer however is equipped with a more powerful engine and a higher speed of the rotors is possible.

Traffic testing of all lanes was carried out using standard Canadian and U.S. Military vehicles. Lugged tires and commercial pattern tires were used at inflation pressures ranging from 15 psi to 70 psi. The lanes capable of carrying the traffic had a minimum density of 0.53 to 0.55 gm/cm^3 and a minimum Rammsonde hardness of 350. The following table shows the percentage of lanes laid by each method which were able to carry the traffic.

TABLE 3.1

Summary of Traffic Tests

Method	Percentage of lanes placed by method indicated which carried traffic
Pulvimixer with heat and rollers	82%
Rollers (segmented and rubber tired) alone	61%
Pulvimixers without heat and with rollers	56%
Pulvimixers alone with heat	7%
Pulvimixers alone without heat	12.5%

In the above analysis, no particular attention was given to such variables as ambient air temperature, temperature of processing, period of age-hardening or hardened snow temperature. However, the analysis strongly indicates that regardless of the method of snow agitation, with or without heat, heavy rollers are essential to produce hard surfaces. Furthermore, whereas the maximum Rammsonde hardness produced without heat with heavy roller was 531, the maximum Rammsonde hardness achieved with heat and with roller was 2631. It can be concluded that the probability of successful lanes where heat and heavy rollers are employed is greater than when heat is not used.

It was reasoned that to produce a snow surface that could "definitely" carry all military traffic, a minimum density of 0.6 gm/cm^3 would be required. It was also confirmed that a density greater than 0.54 gm/cm^3 was very difficult to achieve by compaction alone, even when using extremely heavy rollers. Therefore the increase in density has to come from a decrease in voids due to the addition of water. The addition of 10.4% by weight of water to snow already compacted to 0.54 gm/cm^3 will bring about the required increase. For a 12-in depth of snow, this represents the addition of 3.3 lb of water per square foot. To satisfy this requirement the following processing schedule was developed.

1. 2 passes with 22,400-lb steel roller - density approaching 0.54 - 0.55 gm/cm^3

2. 5 passes of pulvimixer with heater (heater output of 2,560,000 Btu/hr, forward speed of 1.9 mph) - 10% moisture added

3. 1 pass of 22,400-lb roller - density increased to 0.56 - 0.60 gm/cm^3

The method described above allows construction of a finished 8-ft roadway (under favourable conditions) to proceed at the rate of 1.9 mph. Diesel fuel consumption is estimated at 233.3 gal/hr.

6. McMurdo Station, Antarctica (1972-73)

A 10 mile test section of snow road, over the Ross Ice Shelf between McMurdo Station and Williams Field, was constructed using a layered compaction procedure. The purpose of the experiment was to simplify the existing cold-processing technique as developed by the Naval Civil Engineering Laboratory (NCEL). The NCEL cold-processing technique has been discussed in Section B of this Chapter under the heading '4. Greenland'.

The simplified snow road construction procedure as outlined by Thomas and Vaudrey [36], consisted of the following steps:

1. Site preparation - The snow surface along the proposed snow road alignment was initially rolled with an 8-ft diameter, 8-ft wide, 10,000-lb steel roller. The rolling was necessary to produce a

fairly uniform, compacted surface for depositing the layers of blown snow.

2. Containment berms - By a single pass along the outer edges of the proposed road, the snowblower deposited 2 berms of snow 24 to 30 inches high. The berms contained the layers of snow subsequently deposited by the blower, and prevented a lateral displacement during the compaction and leveling of the individual layers.

3. Constructing the snow layers - Snow was deposited between the containment berms as evenly as possible and in sufficient quantity so as to produce a 4-in layer after leveling and compaction had been completed. Leveling of the blown snow, immediately following the deposition, was attempted with low ground pressure (LGP) D-4 and D-8 dozers, however, with no success. It became necessary to use an 80-ft snowplane, towed by an LGP D-4 dozer, to accomplish the leveling.

To compact the 4-in layers, 3 walking passes of the LGP D-8 tractor were used. Attempts to use the 10,000-lb roller were unsuccessful as the roller tended to plow creating a rough and humpy surface.

4. Preparing finished surface - Once the desired road height was achieved, the 80-ft snowplane was used for finish leveling the surface. After finish leveling, the road was allowed to set up for 3 days. Then to surface harden the snow road a rubber-tired, wobbly-wheeled roller was used as in the conventional NCEL cold-processing method. Following the rolling, a timber drag was towed by a 1-ton pickup to smooth the road surface. After 4 days of age hardening, the road was opened to normal traffic.

The study concluded that roads built by the modified method would give satisfactory service for the movement of cargo and personnel by heavy, wheeled transportation equipment. Test results have shown that the densities and shear strengths obtained by the layered method compare favourably with those obtained by the conventional cold-processing method (Pulvimixing). Furthermore, the layered method allows a reduction in overall construction time by more than 40 percent and eliminates the need for special equipment such as the ski-mounted snow mixer.

7. Norman Wells, N.W.T.

During March and April of 1973, a winter road research study was conducted (Adam [2]) near Norman Wells, N.W.T. to evaluate construction methods and environmental effects of various types of winter roads. The research study included the construction and trafficking of a compacted snow road, an ice-capped snow road, and a solid ice road. The evaluation of the winter roads, as regards to construction method and trafficability, are summarized.

1. Snow Road - Snow was first bladed in towards the centerline of the right-of-way to form about a 30-ft wide base for the snow road. A makeshift leveler-compactor was devised (as more adequate equipment was not available at the site) using a large diameter log with a Euclid tire tied on for added weight. This leveler-compactor was towed by a D-7-17A tractor and 2 complete passes over the road surface were performed. The snow road was allowed to age-harden for 1 day before it was processed to a depth of 10 inches using a disc tiller. To permit control over the depth of penetration, the disc tiller was mounted to the front-end loader assembly of a IHC-TD6. The snow road

was processed by 2 passes of the disc tiller and then compacted by 4 passes of a D-7 tractor, each pass covering the road surface track-to-track. The road was allowed to age-harden for 2 days before it was traffic tested to destruction.

Prior to the traffic testing, the snow road had a density of 0.53-0.54 gm/cm^3 and a Rammsonde hardness of 251. In one lane, the snow road failed beyond repair after 25 passes of a Fargo, B-30 series, 15-passenger bus with a GVW of 7,700 lb, and tire inflation pressure of 29 psi. In the other lane, the snow road failed beyond repair after 4 passes of a 65,000 lb, FWD, 6-wheel drive water tank truck. The traffic tests support the earlier studies carried out at Kapuskasing, Ontario where it was determined that a minimum Rammsonde hardness of 350 was required before a snow road could be trafficked by wheeled vehicles.

2. Ice-capped snow road - The snow road of 1. was reshaped and then compacted in 4 walking passes of a D-7 tractor. This was followed with an additional 4 passes of the leveler-compactor. The road surface was finally leveled with a single pass of an I-Beam drag. The I-Beam drag consisted of 6 I-beams (18 in x 7 in x 7 ft) arranged in a V-shape with 3 I-beams hooked one behind the other per side. The snow density attained was 0.50 gm/cm^3 over an average road thickness of 37 cm and the average Rammsonde hardness after 23 hours of age-hardening (in an ambient temperature of approximately -10°F) was 75.

Approximately 24 hours after the reshaping and compacting of the snow road was completed, water was applied at the rate of

0.49 gal/ft^2 by hose. The density of the ice-capped snow road averaged 0.63 gm/cm^3 over a 20-cm thickness, 0.79 gm/cm^3 over a 10-cm thickness, and 0.85 gm/cm^3 over a 5-cm thickness. After 12 hours of age-hardening, the average Rammsonde hardness increased to 646.

One day after the ice-capping, the ice-capped snow road was traffic tested. After 25 passes of the Fargo 15-passenger bus, minor failures were observed along the outer edges of the road surface. During further trafficking, numerous more failures (2.5% by area) occurred. These failures were easily repaired by hand and the road remained serviceable on a continuous basis. The occurrence of weak spots was attributed to the lack of uniformity attained by the hose-end method of water application.

The traffic testing remained more or less continuous from March 15 to April 1. The test vehicles included:

1 Fargo, 15 passenber bus, GVW 7,700 lb., tire pressure 29 psi;

1 Fargo 4 x 4 Crew Cab, GVW 8,000 lb., tire pressure 40 psi;

1 Ford tandem T804 Series, GVW 43,000 lb., tire pressure 65 psi;

1 IHC-100 Series, GVW 5,400 lb., tire pressure 28 psi;

2 GMC tandems, GVW 39,000 lb., tire pressure 80 psi;

1 Ford F-500, GVW 20,000 lb., tire pressure 75 psi;

1 Ford F-350, GVW 10,000 lb., tire pressure 60 psi; and

1 Ford F-100, GVW 5,000 lb., tire pressure 32 psi.

A total of 35,924 vehicle passes were accomplished by these vehicles travelling an estimated 8,160 miles over a 1,200-ft test loop.

The test loop included the ice-capped snow road and an ice road. The ice road portion of the test loop is discussed next.

3. Ice road - A road bed was prepared by an initial leveling operation using the Euclid tire drag towed by the D-7 tractor. The ice road was then constructed by spraying water from a spray bar mounted on the back of the water tank trucks. By successive applications of water, an ice layer was built up to an approximate thickness of 5.35 inches (13.5 cm). As already noted, the ice road portion of the test loop was trafficked at the same time as the ice-capped snow road. The ice road held up well to the traffic, requiring little maintenance except for occasional sanding to improve traction.

The study makes several concluding comments regarding the 3 types of winter roads evaluated. These are summarized as follows:

- Unless sufficient moisture is available in the snow it is impossible to construct a trafficable snow road without the use of heavy drags and rollers. Even with sufficient moisture the use of light equipment is questionable.
- Application of 0.5 to 0.8 gal/ft^2 of water to a minimally constructed snow road will produce a trafficable ice-capped snow road overnight if temperatures are well below freezing. Maintenance of ice-capped snow roads is substantial if the hose-end method of water application is used. It is possible that by a more uniform application of water, a large portion of the maintenance could be eliminated.
- Ice roads may be trafficked before completion on a limited basis. No traffic, however, could be tolerated on a snow or ice-capped snow road during its construction.

- The large quantities of water required for ice road construction may prohibit extensive use of this type of winter road.

- The traffic applied to the test loop, as regards to total number of passes and total tonnage, simulates the actual traffic anticipated in 48" pipeline construction.

Final Comment

It is apparent that a number of "interrelated" factors will influence winter road construction practice. These include: geographic location; meteorological conditions; building material properties; structural requirements; and other multi-disciplinary concerns (environmental, etc.). In order to adapt a technique of winter road construction to the requirements, something must be known about the range of results obtained by the different construction methods and the variation in results under various conditions.

In the review (Construction Methods and Results), two phases in the field of winter road research can be distinguished. The first phase includes: fundamental studies on the properties and behaviour of snow; the securing of information on the variations of the bearing properties under different conditions; and the determination of the demands made on the snow substratum by the different types of transport. The second phase belongs to the category of applied research and is aimed at the development of construction and maintenance techniques that satisfy the requirements from the viewpoint of traffic demand, economy, and environmental impact. The literature indicates that although the first phase is fairly well developed, the second is still in its adolescent stages.

CHAPTER IV

FIELD STUDIES

The field studies were performed with the following primary objectives:

1. To evaluate the performance of a Sicard snow blower as a snow processing implement.
2. To study the effects of ambient and snow temperatures on Rammsonde hardness.
3. To investigate the potential of utilizing a tow-type surface heater in the construction of snow roads.

The construction equipment was provided by the University of Manitoba Maintenance Department. The limited equipment selection determined the course of the field studies.

A. EXPERIMENTAL TECHNIQUES

Construction of Snow Road Test Lanes

In order to evaluate the performance of the Sicard snow blower as a snow processor, 5 snow road test lanes were constructed. Three of the test lanes (200 ft long and 18 ft wide each), were constructed end-to-end using 2, 4 and 6 complete blower passes (Jan. 26/76). Two more lanes (350 ft long and 12 ft wide, each), were constructed separately (Jan. 26/76 and Mar. 18/76) using a single processing.

Sufficient snow was brought in and positioned adjacent to the roadbed by windrowing the snow on either side of the proposed roadway with a Champion D-562D motor grader. The positioning was necessary as the snow blower was equipped with a standard loading chute and could not eject the snow to the rear of the machine, only to the side. Immediately following the windrowing, the snow was processed and deposited adjacent to the windrow if further processing was to be performed, or spread as uniformly as possible over the roadbed surface if the final processing was being completed. The snow blower was kept at full load, moving at a forward speed of 60 ft /min , with an output of about 630 tons of snow per hour. The auger and impeller speed was maintained at about 700 r.p.m. Photographs E-1 to E-6 illustrate the construction procedure.

Following the final processing and deposition, the road surfaces were smoothed and dragged with a 6" x 10" x 11' wide-flange, steel beam in 8 complete passes each. Further compaction was attempted with a Case 1150 crawler following a 2-hour period of age-hardening (Jan. 26/76). A 4-ft diameter, 2-ton, steel roller was used in constructing the single processed test lane on March 18/76.

Surface Compaction at 0°C (Feb. 9/76)

During the period January 26/76 to March 18/76, unusually high temperatures were experienced. During one of the warm spells, the snow temperature climbed to 0°C, simulating a surface condition as might be produced by a surface heater. During this warm period, a portion of the single-processed test lane was surface compacted with the Case 1150 crawler tractor. The ground pressure delivered by the tractor tracks was about 9 psi.

Rammsonde Hardness Tests

The snow road hardness in the 0 - 5 cm , 5 - 10 cm , 10 - 15 cm , and 15 - 20 cm , layers was observed daily, starting immediately after construction and continued up until permanent thaw in March. The 1360 readings obtained were used as indicators as regards to road bearing strength, with high and low Rammsonde hardness corresponding to high and low strength respectively. The Rammsonde cone penetrometer is discussed in detail in Appendix C.

The snow hardness of the different lanes was compared and the significance of single- and multiple-processing using the snow blower, was evaluated. The age-hardening phenomenon and the temperature/hardness relationship in the test lanes was observed. The correlation between snow temperature and hardness was determined and a linear regression equation fitted to the data. The analysis involved 700 snow temperature/hardness data pairs.

Temperature

Air temperatures were observed on a continuous basis for the duration of the field studies. The proximity of the field test area to the Meteorological Station at the Winnipeg International Airport, permitted filling in of missing data from the published monthly Meteorological Summary. The daily relative humidity for the testing period was derived from the same source. Snow road temperatures were observed only during the time of Rammsonde testing and were taken at a 10-cm depth.

Grain Size

The grain size of the snow, before and after processing, was estimated by visual inspection using a millimeter scale. The snow was randomly sampled and an apparent average particle size determined. No statistical interpretation was applied to the sampling and no sieve analysis was performed to establish the particle-size distribution.

Density

A snow sampling tube was used in determining the average density of the undisturbed and reconstituted snow. The snow cores measured 5 cm in diameter and 19 cm (max.) in length and the average mass density (gm/cm^3) was determined by weighing the known volume of snow. The density of the individual test lanes was based on the mean of 6 core samples in each lane.

The density 'profile' in a total of 34 core samples was determined (prior to and after the burn test) using a Nuclear-Chicago 8775 scaler/timer, and a Harshaw DS-200 crystal scintillation detector. Cobalt-60 was used as a gamma-ray source which was directed as a beam through a pin-hole in the machined lead shielding bricks. The core sample was placed between the radioactive source and detector and at least 10 counts of 0.2-minute duration were made at each point along the core. The procedure is presented and evaluated in Appendix D.

The Prototype Wood-fired Surface Heater

The good results obtained from the snow road surface compaction test at 0°C encouraged an investigation into the possibility and practicability of artificial surface heating. For this purpose a wood-fired heater was considered to be potentially the most advantageous. That is, along with performing its primary function, the heater would also provide a disposal facility for right-of-way slash material. To evaluate the potential of the heating method, a prototype heater was constructed and tested.

Six, 45-gal , oil drums were cut in half longitudinally and the halves were welded together in a configuration as shown in Figure E-1 of

Appendix E. The assembly was adequately reinforced and tow hooks were provided as shown. The weight of the heater, as constructed, was 550 lbs.

Seasoned pine was selected as the fuel for the burn tests and one (1) cord of the seasoned wood was used. The wood was randomly piled in the burner and after setting it on fire, 15 minutes was allowed for the fire to spread evenly to all parts of the pile. The wood burner was then towed by the Case 1150 crawler over the multiple-processed snow road.

The slowest tow speed possible with the crawler was 20 ft/min. To study the effects of the heating at speeds less than 20 ft/min , a start-stop towing procedure was necessary. During the stop intervals, the heater was held stationary for 1, 2, 4, 6, 8, 12 and 20 minute durations.

B. RESULTS AND DISCUSSION

Construction of Test Lanes

After the final snow processing and deposition by the blower, the snowbed varied in depth from 1.5 to 3.0 feet (Photograph E-3). This depth of snow proved excessive for the equipment used and maneuverability problems were encountered. During the leveling and dragging operation, the crawler tended to bog down churning up the snowbed rather than compacting it. Also, the steel drag was too light and unstable to be very effective. With each successive pass of the crawler and drag combination, the snowbed became increasingly spread out and uneven. It became necessary to re-shape the snowbed with the grader and start anew. This time, the leveling was achieved by using two tow vehicles, one on each side of the roadbed with the steel drag in the middle. This gave some stability to the drag and a smooth and even road surface was achieved in 8 passes. Compaction of the snow road was negligible by this dragging method.

Two hours after completion of the 2, 4 and 6 blower-pass test lanes an attempt was made at compacting the roads by walking the Case 1150 crawler over the road surfaces. As it turned out, age-hardening had not advanced sufficiently and the tractor broke through the road surface on the first pass. It was observed that the double-processed road section carried the tractor with no difficulty whereas the tractor immediately broke through on the 4 and 6 blower-pass test lanes. Since it is logical to expect a finer particle size to be produced by repeated processing, the observation suggests a slower age-hardening response in finer snow. Ager [4] reports similar observations regarding hardness sensitivity to temperature and grain size. The hardness/temperature/ grain-size interrelationship is discussed further in later sections.

Construction of the single-processed test lane (March 18/76) using the 2-ton, 4-ft diameter steel roller, was unsuccessful. To avoid the maneuverability problems previously experienced, a layered compaction procedure was attempted. It was found that even with shallow snow layers of 3 to 4 inches, a competent road could not be constructed. Although the reduction in snow depth improved equipment maneuverability significantly, the performance of the steel roller remained unacceptable. Due to the small roller diameter, skidding tended to occur producing an uneven bumpy surface. Furthermore, with the roller width and diameter being approximately equal, a side-to-side tipping action persisted. After 2 or 3 passes of the roller, all resemblence of a roadbed was destroyed. The present experience, with blower-processed snow, lends justification for the use of specially designed long-span snow planes such as recommended by Thomas and Vaudrey [36], (McMurdo Station, Antarctica).

Porosity, Density and Grain Size

The minimum porosity obtainable with an aggregate of 'equidimensional' particles, all touching one another is 40.2%. This corresponds to a snow density of approximately 0.53 gm/cm^3. Recalling that a snow road density of 0.6 gm/cm^3 has been established as the acceptable minimum (U.S. - Canadian Joint Compaction Trials [38]), the premise upon which blower-processing is based, is that the required density can be accomplished by a filling of the void spaces with particles smaller than those creating the voids. That is to say, the milling and mixing action of the snow-blower produces a particle size distribution such that the physical condition of optimal close packing is approached. This condition, in addition to satisfying the density requirement would also be most advantageous for maximum bond (strength) growth. Unfortunately, as will be seen in the following discussion, the field observations permit only a qualititive evaluation of the cold-processing technique.

The average density of the 1, 2, 4 and 6 blower-pass test lanes was 0.458, 0.481, 0.511 and 0.512 gm/cm^3 respectively (Table A-3, Appendix A). A 5% gain in density was achieved by increasing the blower-processing from 1 to 2 passes and a further 6% gain by increasing the processing from 2 to 4 passes. Repeated processing beyond 4 passes, produced no further density increase. The apparent average grain size before and after processing, was estimated at 2 mm and 0.6 mm, respectively. No visual difference was detectable in the single- and multiple-processed snow.

Failure to achieve densities that approach the acceptable 0.6 gm/cm^3 can be attributed, at least in part, to inadequate compaction of the processed snowbed. However, without knowledge of the particle-size gradation in the processed snow, the effectiveness of the processing method remains uncertain. In this regard, the hypothesis is adopted that repeated processing tends to produce an 'equidimensional' material with no significant decrease in the average size of the snow particles. As the present density results imply, the condition of minimum porosity, produced by a close packing of equidimensional particles, is approached through the repeated processing. Previous studies lend further credence to the hypothesis in that they show repeatedly, that regardless of the intensity of agitation, a snow density of approximately 0.53 gm/cm^3 remains the upper limit. Although, in concept, the snow processing in the present field studies was performed to achieve non-uniformity in grain size, the results make strong claim that an equidimensional particle size was produced.

Performance Characteristics of the Sicard Snow Blower

At full load, the Sicard snowblower (powered by an IHC-345, V-8 engine), processed the freshly windrowed snow at an average rate of 630 tons per hour. At a full depth of cut (blower intake hood, 78" x 30") and an impeller speed of 700 r.p.m., a forward speed of about 60 ft/min (0.68 m.p.h.) could be maintained. The density of the windrowed snow was approximately 0.30 to 0.35 gm/cm^3.

The discharge characteristics and spreading uniformity (photograph E-3) depended on the machine operator's ability to maintain a constant load on the intake augers. Overloading or 'choking' occurred frequently, requiring temporary stops so that engine and impeller r.p.m.'s could be regained. This behaviour predominated when double-depth processing (see Chapter III, '4. Greenland') was attempted.

Rammsonde Hardness of Test Lanes

The Rammsonde hardness data are presented in Appendix A. The hardness numbers are given in both the uncorrected (conventional) and corrected forms. The two methods of presentation are used in Figure A-1 to illustrate the typical snow road hardness obtained.

The hardness data indicate very low strength in the snow roads. In fact, for all 'practical' purposes, none of the snow roads could be classified as trafficable. On the basis of previous investigations, in particular the experience gained at Kapuskasing, Ontario [38], and the studies by Adam [1,2], an average hardness in excess of *350 is required. On the basis of this criterion, only the test lane compacted at the surface temperature of 0°C was acceptable. Figure A-4 illustrates the hardness increase due to the surface compaction.

A distinction between 2, 4 or 6 blower-pass processing could not be made on the basis of the Rammsonde hardness data, although, the single-processed lane (without surface compaction at 0°C) showed some tendency to be softer. It was generally observed, however, that with an increase in hardness (decrease in temperature), the deviation from the mean increased as well.

Rammsonde Hardness-Temperature Relationships

The relationship between Rammsonde hardness and air temperature, for the duration of the testing period, is shown in Figure A-2. It is observed that during the initial age hardening period (approx. 2 days), the snow road hardness increased independently of the fluctuation (+ or −) in air temperature. After that, with some lag however, the hardness paralleled the variations in air temperature. In numerous previous attempts, no correlation between Rammsonde hardness and air temperature was found. This is likely due to this 'lag' phenomenon where consequently the handling of data near the temperature inflection points becomes

---

* The average Rammsonde hardness of 350 is equivalent, in the corrected form, to an average hardness of 1050 in the top 10 cm.

problematical.

In the present study, correlation of Rammsonde hardness and snow road temperature was attempted. The correlation coefficients found for the 0-5 cm, 5-10 cm, 10-15 cm and 15-20 cm depths were 0.78, 0.65, 0.43 and 0.37, respectively. A data scatter diagram and regression line, for the 0-5 cm layer is represented in Figure A-3.

Burn Tests

As a means of increasing snow density, the filling of void spaces, with free moisture through surface heating, was investigated. The results of the burn tests, using the prototype surface heater, are given in Appendix B. Figure B-1 shows the snow road density profiles, before and after the heat application.

The practicability of the heating method may be appraised in terms of efficiency. For the present analysis, efficiency is defined as follows:

$$e = \frac{\text{(Energy theoretically required to achieve the observed density increase)}}{\text{(Total energy expended during the burn interval)}}$$

The results indicate that the heating method is about 0.5% efficient. The low efficiency is attributable to two factors. Firstly, the design of the heater permitted large quantities of heat to be lost to the atmosphere, and secondly, as indicated by the efficiency equation, the density increase depended entirely on the generation of free water to occupy the pore spaces. Clearly, surface heating in this fashion becomes only a poor substitute for the direct water application method.

Once the snow is warmed to 0°C, the additional heat applied to the snow mass is used for conversion of the snow to the liquid state.

The compaction test at 0°C (previously discussed), indicates that a high moisture saturation, even with minimal compaction, is not required to produce a trafficable pavement. A significant improvement in results can be expected through the combination of surface heating immediately followed by heavy compaction.

An obvious and essential modification to the prototype heater would be the addition of a suitable canopy over the heating unit. Appurtenant features may include a fan and soot trap. As indicated in Photograph E-8, the containment of soot and ash particles would be a major consideration.

A sample calculation of the heating efficiency just discussed is presented in Appendix B.

CHAPTER V

CONCLUSIONS AND RECOMMENDATIONS

The literature review in this study identified two distinct areas of research pertaining to snow. One area of research deals with the theoretical aspects of the snow properties and the other with the practical applications of snow as an engineering material. Evidently, the two areas have evolved more or less independently and thus much of the present practical knowledge regarding snow roads is based on judgemental observation. Although the more recent studies have generally been based on evaluable data, many of the conclusions have been drawn on the sheer weight of accumulated experience.

By virtue of its vast implications, the single most important factor influencing snow road construction is geographic location. Implicit are the influences of meteorological conditions, terrain features, environmental stability, ... etc. The technical or procedural aspects specific to the present study are dealt with below.

The results of the field studies indicate that regardless of the method or intensity of snow processing, heavy compactors are essential for compaction of the snowbed. If heavy rollers are used, they must be of large diameter in order that free rolling can be maintained. When dealing with blower-processed snow, it appears that a layered-compaction procedure, as proposed by Thomas and Vaudrey [36] is necessary. Depending on the type and size of construction equipment used, the fine-grained snow produced by blower processing may create mobility problems even in snow depths of 4 or 5 inches. The use of containment berms would eliminate the problems of lateral displacement during leveling and compaction.

Multiple-processing, using the Sicard snow blower, tended to produce snow with an equidimensional particle size ($\approx$ 0.6 mm). No significant decrease in the average particle size or increase in strength (hardness) was observed with repeated processing. Apparently, the benefits attributable to processing result largely from the sintering phenomenon which is enhanced by the mixing of fine snow particles of different temperature.

The results of the snow road age-hardening observations confirmed the findings of previous studies. For the first 48 hours (approx.) after the snow has been reconstituted, an increase in hardness will continue regardless of the fluctuation (+ or -) in temperature. After that, there appears to be a strong correlation between snow hardness and snow temperature. In the field studies, where the snow temperature data were not entirely adequate, a correlation coefficient of 0.78 was found for the top 5 cm of the snow roads.

The results of the compaction and burn tests indicate that a combination of surface heating and surface compaction may be a practical means of increasing snow road density. Surface heating alone, however, is only a poor substitute for the direct water application method where in both cases the increase in density is due exclusively to the introduction of free water into the pore spaces. Modifications, to minimize heat loss are necessary before further testing of the wood-fired heater would be practical. A canopy, which may include a fan, a heat discharge chute and a soot trap are essential.

Unquestionably, continued field investigations will contribute to the present snow road construction 'know-how'. Future studies should include:

1. A detailed investigation into the particle-size gradation produced by the different methods of snow processing.
2. Full-scale field tests utilizing improved versions of the wood-fired surface heater in combination with roller compaction.
3. Further investigations into the relationship between snow hardness and snow temperature.
4. Development of a 'standard' field snow-testing kit and data documentation procedure. The testing equipment must include practical devices by which actual grain size and arrangement can be studied. Also, temperature recording devices which could be permanently installed through a cross-section of snow road.
5. Documentation, by interview, of unreported construction experience. It is expected that from these interviews will emerge avenues of investigation which otherwise might not be uncovered.

BIBLIOGRAPHY

[1] Adam, K.M., Winter Road Study, Prepared for the Environment Protection Board, Sponsored by Canadian Arctic Gas Study Ltd., Winnipeg, Manitoba, 1972.

[2] Adam, K.M., Normal Wells Winter Road Research Study, to Canadian Arctic Gas Study Ltd., Interdisciplinary Systems, Ltd., Winnipeg, Manitoba, 1973.

[3] Adam, K.M., Wilson, T.M., The inter-relationships of water application rate, ambient temperature, snow road properties and ice-cap depths during the construction of winter roads, Dept. of Civil Engineering, University of Manitoba, A Research Report to Canadian Arctic Gas Study Limited, 1975.

[4] Ager, B.H:son, Some tests on the compactibility and hardness after compaction of different types of snow, Journal of Galciology, 1964.

[5] Ager, B.H:son, Compacted snow as a transport substratum, National Research Council of Canada, Tech. Trans. 865, Ottawa, Canada, 1956.

[6] Bader, H., The physics and mechanics of snow as a material, U.S. Army Cold Regions Research and Engineering Laboratory, Research Report, Hanover, New Hampshire, 1962.

[7] Benson, C.S., Trabant, D.C., Field measurements on the flux of water vapour through dry snow, The Role of Snow and Ice in Hydrology Symposium, Vol. 1, 291-298, UNESCO-WMO-IAHS, 1973.

[8] Camm, J.B., Snow-Compaction Equipment, Snow drags, Tech. Report 109, U.S. Navy Civil Engineering Laboratory, Port Hueneme, California, 1960.

[9] Clark, E.F., Abele, G., Wuori, A.F., Expedient snow airstrip construction technique, U.S. Army Cold Regions Research and Engineering Laboratory, Research Report, Hanover, New Hampshire, 1973.

[10] Colbeck. S.C., One dimensional water flow through snow, U.S. Army Cold Regions Research and Engineering Laboratory, Research Report 296, Hanover, New Hampshire, 1971.

[11] Colbeck, S.C., Effects of stratigraphic layers on water flow through snow, U.S. Army Cold Regions Research and Engineering Laboratory, Research Report 311, Hanover, New Hampshire, 1973.

[12] Colbeck, S.C., Theory of metamorphism of wet snow, U.S. Army Cold Regions Research and Engineering Laboratory, Research Report 313, Hanover, New Hampshire, 1973.

[13] Colbeck. S.C., The capillary effects on water percolation in homogeneous snow, Journal of Glaciology, Vol. 13, No. 67, 85-97, 1974.

[14] Colbeck, S.C., Water flow through snow overlying an impermeable boundary, Water Resources Research, Vol. 10, No. 1, 119-123, 1974.

[15] Colbeck. S.C., Analysis of hydrologic response to rain-on-snow, U.S. Army Cold Regions Research and Engineering Laboratory, Research Report 340, Hanover, New Hampshire, 1975.

[16] Colbeck, S.C., A theory for water flow through a layered snowpack, Water Resources Research, Vol. 11, No. 2, 261-266, 1975.

[17] Combarnous, M.A., Fried, J.J., Dispersion in Porous Media, Advances in Hydroscience (V.T. Chow, ed.), Vol. 7, 169-280, Academic Press, New York, 1971.

[18] de Quervain, M.R., Snow structure, heat, and mass flux through snow, The Role of Snow and Ice in Hydrology Symposium, Vol. 1, 203-223, UNESCO-WMO-IAHS, 1973.

[19] Diamond, M., Studies on vehicular trafficability of snow (Part 1) Arctic Institute of North America, April 1956.

[20] Easton, R., Navy snow-compaction equipment. Military Engineer 1964, Vol. 56, No. 372, 417-419.

[21] Eriksson, R., The compacted snow road I, Properties of snow, National Research Council of Canada, Tech. Trans. 849, Ottawa, Canada, 1959.

[22] Friesen, D., A study of snow as a porous medium, Unpublished undergraduate Civil Engineering Thesis, University of Manitoba, April 1974.

[23] Giddings, J.C., LaChapelle, E., The formation rate of depth hoar, Journal of Geophysical Research, Vol. 67, No. 6, 2377-2383, 1962.

[24] Kuriowa, D., Liquid permeability of snow, Low Temp. Sci., Ser. A, Vol. 26, 29-52, 1968.

[25] Laliberte, G.E., Fluid Mechanics of Unsaturated Porous Solids, Course outline for 34:704, Dept. of Agricultural Engineering, University of Manitoba, Winnipeg, Manitoba 1970.

[26] Leijonhufvd, A.D:son, The compacted snow road III, Field tests and practical applications, National Research Council of Canada, Tech. Trans. 909, Ottawa, Canada, 1955.

[27] Luikov, A.V., Heat and Mass Transfer in Capillary-porous Bodies, Pergamon Press Ltd., London, 1966.

[28] Male, D.H., Norum, D.I., Besant, R.W., A dimensional analysis of heat and mass transfer in a snowpack, The Role of Snow and Ice in Hydrology Symposium, Vol. 1, 258-290, UNESCO-WMO-IAHS, 1973.

[29] Martinelli, M., Jr., Physical properties of alpine snow as related to weather and avalanche conditions, U.S. Dept. of Agriculture, Forest Service, Research Paper RM-64, 1971.

[30] Mellor, M., Polar snow - A summary of Engineering Properties, Ice and Snow, Ch. 36, Proceeding of Conference, MIT, (W.D. Kingery, Ed.) MIT Press, Cambridge, Massachusetts, 1963.

[31] Moser, E.H., Jr., Navy cold-processing snow-compaction techniques, Ice and Snow, Ch. 34, Proceedings of Conference, MIT, (W.D. Kingery, ed.), MIT Press, Cambridge, Massachusetts, 1963.

[32] Moser, E.H. Jr., Roads on snow and ice, Symposium on Cold Regions Engineering, Alaska Section of ASCE and Univ. of Alaska, Vol. 1, Univ. of Alaska, 1971.

[33] Muclear-Chicago Corp. Nuclear-Chicago laboratory manual (Lab. Scaler Model 8775), Pub. No. 713910, Des Plaines, Illinois, 1966.

[34] Nuttall, C.J., Thompson, J.G., A study of some phases of the snow/vehicle interaction, Defence Research Board, Report No. DR 127, Ottawa, Canada, 1958.

[35] Putkisto, K., Snow as a road-building material, National Research Council of Canada, Tech. Trans. 822, Ottawa, Canada, 1959.

[36] Thomas, M.W., Vaudrey, K.D., Snow road construction technique by layered compaction of snowblower processed snow, Naval Civil Engineering Laboratory, Tech. Note N-1305, Port Hueneme, California, 1973.

[37] Veda, H., Sellmann, P., Abele, G., USA CRREL Snow and Ice Testing Equipment, Special Report 146, U.S. Army Cold Regions Research and Engineering Laboratory, Hanover, New Hampshire, 1975.

[38] U.S. - Canadian Joint Compaction Trials, Report on snow compaction trials, Winter 1952-1953, DRB/BSIS Documents, 125 Elgin Street, Ottawa, Canada, 1953.

[39] U.S. Navy Snow-compaction equipment, Snow rollers, Tech. Report 107, U.S. Navy Civil Engineering Laboratory, Port Hueneme, California, 1961.

[40] U.S. Navy Arctic Engineering, Tech. Publ. NavDocks TP-PW-11, Dept. of the Navy, Bureau of Yards and Docks, Washington 25, D.C., 1955.

[41] Waterhouse, R., Re-evaluation of the Rammsonde hardness equation, Special Report 100, U.S. Army Cold Regions Research and Engineering Laboratory, Hanover, New Hampshire, 1966.

[42] Welty, J.R., Wicks, C.E., Wilson, R.E., Fundamentals of Momentum, Heat and Mass Transfer, John Wiley and Sons, Inc., New York, 1969.

[43] Wuori, A.F., Supporting capacity of processed snow runways, U.S. Army Cold Regions Research and Engineering Laboratory, Tech. Report 82, Hanover, New Hampshire, 1962.

[44] Yen, Y.C. Recent studies on snow properties, Advances in Hydroscience (V.T. Chow, ed.) Vol. 5, 173-214, Academic Press, New York, 1969.

APPENDIX A

RAMMSONDE HARDNESS DATA AND OBSERVATIONS

TABLE A.1

Summary of Rammsonde Test Results

Note: - Rammsonde hardness values corrected as indicated by Veda, Sellman, Abele [37] are shown in brackets. (see Appendix C)
- * identifies lane with surface recompacted at snow temperature of 0°C.

Date	Time	Age Hardening Hours (Days)	No. of Blower Passes	Rammsonde Hardness No. 0.5 cm.	5-10 cm.	10-15 cm.	12-20 cm.
Jan.26	17:00	2.5(0.1)	1	23(107)	31(49)	-	-
			1	15(69)	31(49)	-	-
			2	31(144)	55(88)	-	-
			2	19(88)	63(100)	-	-
			4	19(88)	63(100)		
	22:00	7.5(0.3)	1	27(126)	35(56)	19	43
			1	27(126)	43(68)	51	51
			2	43(201)	75(120)	67	51
			2	43(201)	59(94)	91	107
			4	39(182)	129(206)	135	207
			4	35(163)	107(171)	75	140
			6	43(201)	99(158)	99	150
			6	43(201)	75(120)	105	63
Jan.27	09:30	18.5(0.8)	1	83(389)	30(48)	48	51
			1	35(150)	91(145)	67	67
			2	35(163)	67(107)	115	203
			2	43(201)	91(145)	139	163
			4	27(126)	43(68)	67	75
			4	43(201)	163(260)	183	153
			6	43(201)	147(235)	211	253
			6	43(201)	163(260)	213	123

TABLE A.1 (continued)

Date	Time	Age Hardening Hours (Days)	No. of Blower Passes	Rammsonde Hardness No. 0-5 cm.	5-10 cm.	10-15 cm.	15-20 cm.
Jan.27	17:00	26.0(1.1)	1	27(113)	67(102)	91	107
			1	27(113)	35(56)	51	67
			2	51(226)	163(260)		
			2	43(201)	99(158)	131	131
			4	43(201)	51(81)	139	123
			4	51(238)	75(120)	139	67
			6	43(201)	107(171)	195	195
			6	43(201)	99(158)	73	43
Jan.28	10:00	43.0(1.8)	1	43(201)	51(81)	83	91
			1	59(276)	67(107)	75	67
			2	51(238)	51(81)	51	115
			2	83(389)	235(376	403	393
			2	83(389)	123(196)	133	233
			4	51(238)	131(209)	93	83
			4	83(389)	163(260)	83	73
			6	75(351)	139(222)	153	173
			6	91(426)	155(248)	213	413
Jan.29	10:00	67.0(2.8)	1	67(314)	67(107)	83	83
			1	107(502)	139(222)	187	187
			2	91(426)	163(260)	283	523
			2	139(652)	187(299)	153	133
			4	91(426)	153(244)	153	213
			4	131(614)	223(356)	183	153
			6	115(539)	323(516)	293	163
			6	123(577)	353(564)	640	640

TABLE A.1 (continued)

Date	Time	Age Hardening Hours (Days)	No. of Blower Passes	Rammsonde Hardness No. 0-5 cm.	5-10 cm.	10-15 cm.	15-20 cm.
Jan.30	16:00	97.0(4.1)	1	83(389)	83(132)	73	83
			1	67(314)	93(148)	113	123
			2	91(426)	75(120)	83	83
			2	107(502)	223(356)	183	173
			4	75(351)	213(340)	213	273
			4	59(276)	73(116)	133	103
			6	91(426)	203(324)	163	213
			6	99(464)	233(372)	313	363
Jan.31	17:00	122.0(5.1)	1	43(201)	43(68)	53	63
			1	43(201)	53(84)	113	123
			2	67(314)	83(132)	83	103
			2	67(314)	93(148)	133	153
			4	67(314)	143(228)	18	15
			4	83(389)	103(164)	133	123
			4	91(426)	183(292)	153	123
			6	83(389)	183(292)	243	263
			6	91(426)	113(180)	73	53
			6	75(351)	113(180)	133	183
Feb. 1	14:00	143.0(6.0)	1	99(464)	173(276)	173	173
			1	131(614)	203(324)	153	73
			2	115(539)	283(452)	193	183
			2	179(840)	283(452)	383	423
			4	179(840)	293(468)	173	133
			4	179(840)	343(548)	193	143
			6	171(802)	503(804)	503	493
			6	235(1103)	213(340)	303	313

TABLE A.1 (continued)

Date	Time	Age Hardening Hours (Days)	No. of Blower Passes	Rammsonde Hardness No. 0-5 cm.	5-10 cm.	10-15 cm.	15-20 cm.
Feb. 2	16:00	170.0(7.1)	1	67(314)	113(180)	163	153
			1	91(426)	163(260)	163	163
			2	131(614)	193(308)	193	163
			2	99(464)	223(356)	403	403
			4	75(351)	153(244)	173	213
			4	99(464)	263(420)	443	503
			6	107(502)	253(404)	603	573
			6	115(539)	203(324)	482	733
Feb. 5	15:00	240.0(10.0)	1	99(464)	163(260)	223	223
			1	82(386)	183(291)	222	290
			2	170(800)	362(679)	932	800
			2	179(840)	603(964)	943	943
			4	136(640)	112(179)	94	166
			4	184(865)	184(295)	184	202
			4	227(1066)	363(580)	263	183
			6	147(690)	433(692)	353	393
			6	82(386)	292(467)	292	252
Feb. 7	12:30	285.5(11.9)	1	50(236)	72(115)	52	72
			1	43(201)	73(116)	103	113
			2	86(405)	112(179)	142	152
			2	63(295)	73(116)	113	143
			4	98(461)	182(291)	322	532
			4	99(464)	293(468)	433	593
			6	76(358)	196(314)	172	196
			6	77(361)	197(315)	197	197

TABLE A.1 (continued)

Date	Time	Age Hardening Hours (Days)	No. of Blower Passes	Rammsonde Hardness No. 0-5 cm.	5-10 cm.	10-15 cm.	15-20 cm.
Feb. 8	16:00	313.5(13.1)	1	35(163)	83(132)	83	113
			1	59(276)	123(196)	203	183
			1	43(201)	83(132)	103	103
			2	77(361)	101(161)	173	221
			2	59(276)	77(123)	53	125
			2	83(389)	223(356)	393	393
			2	75(351)	143(228)	183	153
			4	77(361)	77(123)	125	101
			4	77(361)	149(238)	149	149
			4	95(445)	149(238)	101	149
			6	77(361)	167(267)	77	113
			6	77(361)	113(180)	113	149
Feb. 9	12:30	334.0(13.9)	1	15(69)	69(110)	123	131
			1	9(41)	57(91)	99	115
			1	15(69)	75(120)	139	147
			1	9(41)	45(72)	59	75
			1	9(41)	93(148)	107	123
			1*	19(88)	43(68)	93	143
			1*	27(126)	103(164)	193	133
			1*	35(163)	153(244)	303	193
			1*	18(88)	93(148)	293	223
			2	15(69)	99(158)	315	303
			2	9(41)	83(132)	263	263
			4	9(41)	103(164)	213	443
			4	9(41)	123(196)	193	123
			6	9(41)	93(148)	153	163
			6	15(69)	103(164)	133	133

TABLE A.1 (continued)

Date	Time	Age Hardening Hours (Days)	No. of Blower Passes	Rammsonde Hardness No. 0-5 cm.	5-10 cm.	10-15 cm.	15-20 cm.
Feb.10	16:00	361.5(15.1)	1	113(530)	194(310)	329	248
			1	95(445)	167(267)	194	140
			1*	473(2222)	653(1044)	545	167
			1*	383(1799)	626(1001)	329	167
			1*	383(1799)	828(518)	193	113
			2	113(530)	221(353)	194	329
			2	113(530)	275(440)	464	464
			4	113(530)	356(570)	275	221
			4	131(614)	275(440)	194	221
			6	131(614)	275(440)	302	302
			6	131(614)	356(569)	356	410
Feb.12	13:15	406.8(17.0)	1	95(445)	146(234)	113	140
			1	77(361)	86(137)	113	95
			1*	329(1545)	680(1088)	275	113
			1*	356(1672)	383(612)	140	113
			1*	275(1291)	248(396)	167	248
			1*	302(1418)	437(699)	275	167
			2	113(530)	194(310)	302	437
			2	95(445)	113(180)	140	113
			4	113(530)	275(440)	275	194
			4	131(614)	194(310)	140	248
			6	149(699)	221(353)	167	32
			6	149(699)	302(483)	410	518
Feb.15	14:30	480.0(20.0)	1	95(445)	140(224)	113	86
			1	77(361)	86(137)	86	86
			1*	329(1545)	545(872)	572	329
			1*	329(1545)	275(440)	113	140
			1*	437(2053)	545(872)	248	140
			2	149(699)	356(569)	329	302
			2	95(445)	140(224)	410	491

TABLE A.1 (continued)

Date	Time	Age Hardening Hours (Days)	No. of Blower Passes	Rammsonde Hardness No.			
				0-5 cm.	5-10 cm.	10-15 cm.	15-20 cm.
			4	95(445)	221(353)	113	86
			4	113(530)	221(353)	167	221
			6	113(530)	194(310)	194	248
			6	113(530)	275(440)	275	221
Feb.16	16:35	506.0(21.1)	1	77(361)	167(267)	113	86
			1	77(361)	86(137)	32	59
			1	59(276)	59(94)	32	86
			1*	302(1418)	464(742)	167	59
			1*	275(1291)	248(296)	113	59
			1*	275(1291)	464(742)	194	59
			2	113(530)	410(656)	464	356
			2	113(530)	140(224)	248	383
			2	77(361)	113(180)	86	113
			4	77(361)	194(310)	194	194
			4	113(530)	221(353)	221	194
			6	95(445)	194(310)	248	329
			6	113(530)	275(440)	410	518
			6	77(361)	140(224)	146	248
Feb.17	13:00	526.5(21.9)	1	59(276)	131(209)	167	167
			1	41(191)	77(123)	77	77
			1	59(276)	59(94)	59	59
			1*	185(868)	221(353)	86	32
			1*	167(784)	221(353)	131	113
			2	77(361)	113(180)	140	221
			2	77(361)	194(310)	140	86
			4	77(361)	194(310)	221	140
			4	59(276)	59(94)	113	194
			4	77(361)	328(526)	275	140
			6	77(361)	328(526)	518	626
			6	77(361)	140(224)	86	221
			6	59(276)	113(180)	248	167

TABLE A.1 (continued)

Date	Time	Age Hardening Hours (Days)	No. of Blower Passes	Rammsonde Hardness No. 0-5 cm.	5-10 cm.	10-15 cm.	15-20 cm.
Feb.19	17:30	579.0(24.1)	1	77(361)	113(180)	140	113
			1	59(276)	140(224)	167	86
			1*	275(1291)	356(569)	248	140
			1*	275(1291)	275(440)	194	140
			2	113(530)	324(526)	437	410
			2	95(445)	167(267)	140	248
			2	58(276)	113(180)	140	113
			4	95(445)	221(353)	167	248
			4	113(530)	167(267)	59	59
			4	77(361)	140(224)	113	221
			6	77(361)	167(267)	194	221
			6	95(445)	194(310)	275	167
Feb.20	17:30	603.0(25.1)	1	59(276)	59(94)	86	86
			1	59(276)	86(137)	86	86
			1	95(445)	194(310)	221	140
			1*	275(2191)	383(612)	167	86
			1*	329(1545)	329(526)	113	86
			2	77(361)	86(137)	113	140
			2	77(361)	86(137)	113	113
			4	113(530)	194(310)	140	140
			4	95(445)	113(180)	221	356
			6	95(445)	140(224)	86	59
			6	131(614)	194(310)	221	221
			6	113(530)	275(440)	464	464
Feb.21	15:15	624.8(26.0)	1	95(445)	194(310)	140	140
			1	94(445)	275(440)	140	140
			1*	329(1545)	356(569)	167	113
			1*	302(1418)	194(310)	140	140

TABLE A.1 (continued)

Date	Time	Age Hardening Hours (Days)	No. of Blower Passes	Rammsonde Hardness No. 0-5 cm.	5-10 cm.	10-15 cm.	15-20 cm.
			2	131(614)	275(440)	356	356
			2	95(445)	113(180)	86	59
			2	113(530)	167(267)	194	194
			4	167(784)	275(440)	410	248
			4	113(530)	86(137)	59	86
			4	95(445)	113(180)	167	194
			6	131(614)	221(353)	194	329
			6	167(784)	248(396)	221	140
Feb.23	16:30	674.0(28.1)	1	77(361)	167(267)	194	140
			1	41(191)	59(94)	113	194
			1	77(361)	59(94)	59	86
			1*	113(530)	410(656)	140	113
			1*	131(614)	572(915)	383	95
			1*	239(1122)	437(699)	302	113
			2	95(445)	113(180)	113	140
			2	77(361)	86(137)	140	113
			4	77(361)	221(353)	221	194
			4	77(361)	221(353)	329	329
			6	77(361)	194(310)	140	167
			6	95(445)	167(267)	221	221
Feb.24	16:00	697.5(20.1)	1	23(107)	41(65)	77	77
			1	41(191)	41(65)	41	41
			1*	248(1164)	680(1088)	464	248
			1*	194(910)	302(483)	140	86
			1*	140(657)	329(526)	140	59
			2	59(276)	275(440)	194	383
			2	77(361)	302(483)	329	464
			4	59(276)	167(267)	167	167
			4	77(361)	221(353)	167	140
			4	77(361)	113(180)	221	167
			6	77(361)	248(396)	221	221
			6	95(445)	140(224)	140	167

TABLE A.1 (continued)

Date	Time	Age Hardening Hours (Days)	No. of Blower Passes	Rammsonde Hardness No. 0-5 cm.	5-10 cm.	10-15 cm.	15-20 cm.
Feb.26	17:00	746.5(31.1)	1	41(191)	59(94)	95	113
			1	59(276)	59(94)	77	77
			1*	275(1291)	248(396)	167	86
			1*	167(784)	140(224)	32	59
			1*	383(1799)	599(958)	545	275
			1*	86(403)	86(137)	113	86
			2	59(276)	167(267)	194	113
			2	77(361)	140(224)	194	113
			4	76(361)	113(180)	86	86
			4	95(445)	95(152)	167	302
			4	77(361)	167(267)	221	140
			6	95(445)	194(310)	194	221
			6	41(191)	167(267)	491	518
			6	77(361)	194(310)	221	302
Feb.29	15:00	816.5(34.0)	1	113(530)	167(267)	113	113
			1	95(445)	140(224)	167	140
			1	77(361)	140(224)	194	86
			1*	248(1165)	572(915)	302	113
			1*	302(1418)	1139(1822)	410	140
			1*	653(3068)	815(1304)	733	221
			2	131(614)	518(828)	653	599
			2	203(953)	464(742)	626	761
			2	149(699)	383(612)	491	599
			4	185(868)	410(656)	410	275
			4	131(614)	302(483)	248	248
			4	167(784)	383(612)	329	248
			6	131(614)	329(526)	275	221
			6	149(699)	383(612)	545	329

TABLE A.1 (continued)

Date	Time	Age Hardening Hours (Days)	No. of Blower Passes	Rammsonde Hardness No. 0-5 cm.	5-10 cm.	10-15 cm.	15-20 cm.
Mar. 4	17:00	914.5(38.1)	1	59(276)	86(137)	86	113
			1	95(445)	113(180)	167	113
			1*	545(2560)	788(1260)	248	86
			1*	491(2306)	491(785)	221	86
			1*	599(2814)	1301(2081)	599	194
			1*	356(1672)	599(958)	248	86
			2	131(614)	410(656)	599	545
			2	131(614)	302(483)	167	140
			2	131(614)	194(310)	140	140
			4	131(614)	248(396)	194	194
			4	95(445)	464(742)	275	167
			6	131(614)	302(483)	221	194
			6	149(699)	275(440)	275	275
Mar. 5	17:00	938.5(39.1)	1	95(445)	167(267)	140	113
			1	77(361)	194(310)	167	113
			1*	410(1926)	545(872)	383	194
			1*	383(1799)	1139(1822)	1058	329
			1*	329(1545)	437(699)	329	221
			1*	410(1926)	923(1476)	572	194
			2	149(699)	383(612)	248	194
			2	113(530)	419(785)	572	329
			2	131(614)	275(440)	221	194
			4	131(614)	302(483)	383	437
			4	131(614)	545(872)	518	250
			6	149(699)	383(612)	356	221
			6	149(699)	410(656)	545	707

TABLE A.1 (continued)

Date	Time	Age Hardening Hours (Days)	No. of Blower Passes	Rammsonde Hardness No. 0-5 cm.	5-10 cm.	10-15 cm.	15-20 cm.
Mar. 7	14:30	984.0(41.0)	1	77(361)	167(267)	194	140
			1	94(445)	167(267)	113	140
			1*	437(2053)	1895(3032)	977	680
			1*	491(2306)	1193(1908)	437	194
			1*	356(1672)	734(1174)	626	356
			2	95(445)	518(828)	680	653
			2	131(614)	437(699)	518	626
			4	131(614)	329(526)	167	248
			4	131(614)	248(396)	221	167
			6	167(784)	491(785)	599	545
			6	113(530)	167(267)	356	194
			6	149(699)	302(483)	248	302
Mar. 9	17:30	1035.0(43.1)	1	59(276)	221(353)	194	140
			1	59(276)	86(137)	59	59
			1	41(191)	140(224)	86	59
			1*	464(2179)	491(785)	221	86
			1*	302(1418)	383(612)	140	140
			1*	329(1545)	896(1433)	545	275
			2	77(361)	167(267)	140	140
			2	131(614)	275(440)	140	113
			4	77(361)	221(353)	59	32
			4	95(445)	248(396)	275	330
			4	77(361)	275(440)	248	167
			6	131(614)	248(396)	302	167
			6	113(530)	356(569)	302	302

TABLE A.1 (continued)

Date	Time	Age Hardening Hours (Days)	No. of Blower Passes	Rammsonde Hardness No.			
				0-5 cm.	5-10 cm.	10-15 cm.	15-20 cm.
Mar.12	12:30	1102.0(45.9)	1	58(273)	112(180)	139	85
			1	76(358)	193(309)	85	58
			1*	328(1542)	760(1216)	247	112
			1*	148(696)	544(871)	328	139
			1*	184(865)	679(1087)	247	112
			2	131(612)	247(395)	220	166
			2	131(612)	490(784)	409	409
			2	131(612)	382(611)	463	382
			4	131(612)	247(395)	166	274
			4	131(612)	220(352)	166	193
			6	112(527)	193(309)	139	139
			6	112(527)	274(439)	220	193

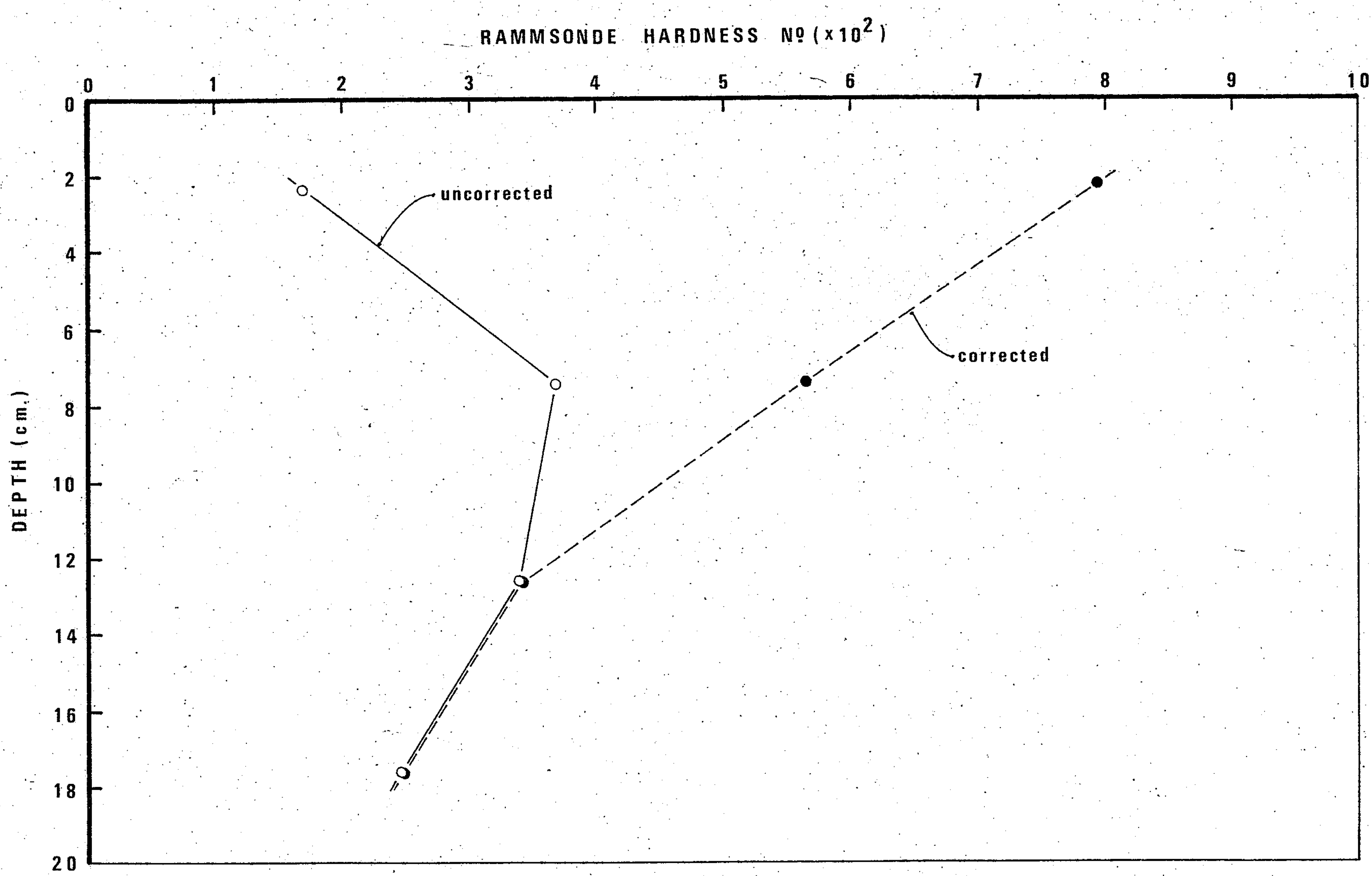

Figure A-1: Typical snow road hardness profiles as indicated by the corrected and uncorrected versions of the Rammsonde hardness data.

TABLE A.2

Summary of air temperature, snow road temperature and relative humidity for duration of Rammsonde testing. (Air temperatures reflect maximum and minimum fluctuations. Snow road temperatures taken at 10 cm depth at time of testing).

DATE	TIME	AIR TEMPERATURE °C	SNOW ROAD TEMPERATURE °C	REL. HUMIDITY % MAX.	MIN.
Jan. 26	08:00	-29.9		86	64
	17:00	-26.0	-16.0		
	22:00	-30.0	-19.0		
Jan. 27	00:00	-28.6		91	65
	09:30	-22.0	-22.0		
	17:00	-12.0	-16.0		
Jan. 28	00:00	- 4.1		89	67
	05:00	3.3			
	10:00	-10.0	- 9.0		
	17:00	-13.9			
Jan. 29	01:00	-20.4		87	72
	10:00	-15.2	-14.0		
	15:00	-11.6			
	21:00	-14.3			
Jan. 30	01:00	-19.7		93	77
	06:00	-15.2			
	16:00	- 9.4	-10.0		
	21:00	- 3.1			
Jan. 31	06:00	- 8.9		93	71
	10:00	- 5.4			
	14:00	1.1			
	17:00	- 5.6	- 6.0		

TABLE A.2 (continued)

DATE	TIME	AIR TEMPERATURE °C	SNOW ROAD TEMPERATURE °C	REL. HUMIDITY % MAX.	MIN.
Feb. 1	00:00	-20.6		79	64
	07:00	-30.4			
	14:00	-22.8	-17.0		
	20:00	-21.8			
Feb. 2	02:00	-20.0		89	77
	10:00	-14.1			
	16:00	-10.1	-11.0		
	22:00	-12.1			
Feb. 3	05:00	-14.0		85	62
	08:00	-14.4			
	14:00	-20.7			
Feb. 4	00:00	-25.6		87	60
	07:00	-28.4			
	14:00	-19.4			
	22:00	-23.8			
Feb. 5	00:00	-26.3		87	71
	08:00	-29.7			
	15:00	-18.1	-19.0		
Feb. 6	00:00	-14.6		78	58
	04:00	-13.8			
	08:00	-17.1			
	16:00	-10.1			
Feb. 7	00:00	-11.1		90	69
	06:00	- 2.2			
	12:30	- 2.0	- 6.0		
	20:00	- 4.1			

TABLE A.2 (continued)

DATE	TIME	AIR TEMPERATURE °C	SNOW ROAD TEMPERATURE °C	REL. HUMIDITY % MAX.	REL. HUMIDITY % MIN.
Feb. 8	02:00	- 8.6		90	76
	10:00	- 6.3			
	16:00	- 1.7	- 5.0		
	22:00	- 0.9			
Feb. 9	04:00	3.8		77	57
	12:30	4.9	0.0		
	20:00	0.6			
Feb. 10	04:00	- 9.5		82	59
	09:00	-13.3			
	16:00	-16.0	-10.0		
	22:00	-23.1			
Feb. 11	07:00	-24.8		88	71
	12:00	-15.5			
	18:00	- 9.2			
Feb. 12	02:00	-12.0		93	75
	08:00	-10.3			
	13:15	-10.0	-11.0		
	20:00	-15.5			
Feb. 13	00:00	-18.1		85	61
	08:00	-17.2			
	17:00	- 9.4			
	22:00	-13.4			
Feb. 14	06:00	- 5.0		90	75
	16:00	- 0.4			
	22:00	- 2.8			
Feb. 15	06:00	- 5.0		93	77
	14:00	- 7.4	- 7.0		
	20:00	- 8.6			

TABLE A.2 (continued)

DATE	TIME	AIR TEMPERATURE °C	SNOW ROAD TEMPERATURE °C	REL. HUMIDITY % MAX.	MIN.
Feb. 16	00:00	-11.0		98	83
	06:00	-15.6			
	16:35	- 2.0	- 8.0		
	22:00	0.0			
Feb. 17	02:00	0.0		100	91
	13:00	0.6	- 5.0		
	18:00	0.0			
Feb. 18	00:00	- 6.8		96	89
	08:00	- 7.2			
	16:00	- 5.6			
	22:00	- 4.4			
Feb. 19	02:00	- 5.0		98	90
	13:00	- 2.1			
	17:30	- 3.0	- 3.0		
Feb. 20	00:00	- 4.9		95	74
	08:00	-16.6			
	14:00	-10.4			
	17:30	-11.6	- 6.0		
Feb. 21	00:00	-16.7		93	70
	08:00	-24.9			
	15:15	-12.1	- 9.0		
	21:00	-10.0			
Feb. 22	02:00	-20.6		93	78
	08:00	-24.6			
	16:00	-12.2			

TABLE A.2 (continued)

DATE	TIME	AIR TEMPERATURE °C	SNOW ROAD TEMPERATURE °C	REL. HUMIDITY % MAX.	REL. HUMIDITY % MIN.
Feb. 23	02:00	- 4.6		90	60
	07:00	- 6.9			
	16:30	3.0	- 7.0		
Feb. 24	00:00	1.2		89	62
	07:00	- 6.1			
	12:00	0.9			
	16:00	3.0	- 6.0		
	22:00	- 1.6			
Feb. 25	02:00	0.0		90	67
	08:00	- 6.5			
	15:00	1.2			
Feb. 26	00:00	2.2		94	69
	12:00	- 5.1			
	17:00	-11.0	- 4.0		
Feb. 27	00:00	-13.8		89	77
	08:00	-11.9			
	18:00	-13.9			
Feb. 28	00:00	-22.7		88	69
	04:00	-27.2			
	12:00	-17.2			
	20:00	-17.8			
Feb. 29	00:00	-21.9		86	62
	07:00	-30.7			
	15:00	-21.8	-15.0		
	22:00	-26.2			

TABLE A.2 (Continued)

DATE	TIME	AIR TEMPERATURE °C	SNOW ROAD TEMPERATURE °C	REL. HUMIDITY % MAX.	REL. HUMIDITY % MIN.
Mar. 1	02:00	-28.8		86	69
	08:00	-28.8			
	19:00	- 8.7			
Mar. 2	00:00	-11.1		91	82
	16:00	- 9.9			
Mar. 3	00:00	-10.8		91	63
	09:00	-20.4			
	16:00	-16.1			
Mar. 4	00:00	-22.0		95	64
	08:00	-24.4			
	17:00	-18.0	-12.0		
Mar. 5	00:00	-28.7		82	61
	06:00	-31.6			
	17:00	-22.0	-17.0		
Mar. 6	00:00	-19.1		87	67
	10:00	-10.7			
	16:00	- 5.6			
Mar. 7	00:00	-12.7		84	63
	06:00	-19.2			
	14:30	- 7.0	-13.0		
	21:00	-11.1			
Mar. 8	01:00	- 9.9		87	66
	06:00	-16.9			
	13:00	- 8.3			
	20:00	-12.2			

TABLE A.2 (continued)

DATE	TIME	AIR TEMPERATURE °C	SNOW ROAD TEMPERATURE °C	REL. HUMIDITY % MAX.	MIN.
Mar. 9	02:00	-12.8		85	66
	10:00	-17.8			
	17:00	-16.0	-10.0		
Mar. 10	00:00	-26.1		86	59
	05:00	-29.6			
	16:00	-13.2			
Mar. 11	00:00	-17.1		89	71
	06:00	-14.3			
	16:00	-11.8			
Mar. 12	00:00	-14.8		86	55
	08:00	-20.1			
	12:30	-13.0	-14.0		
	17:00	- 9.8			

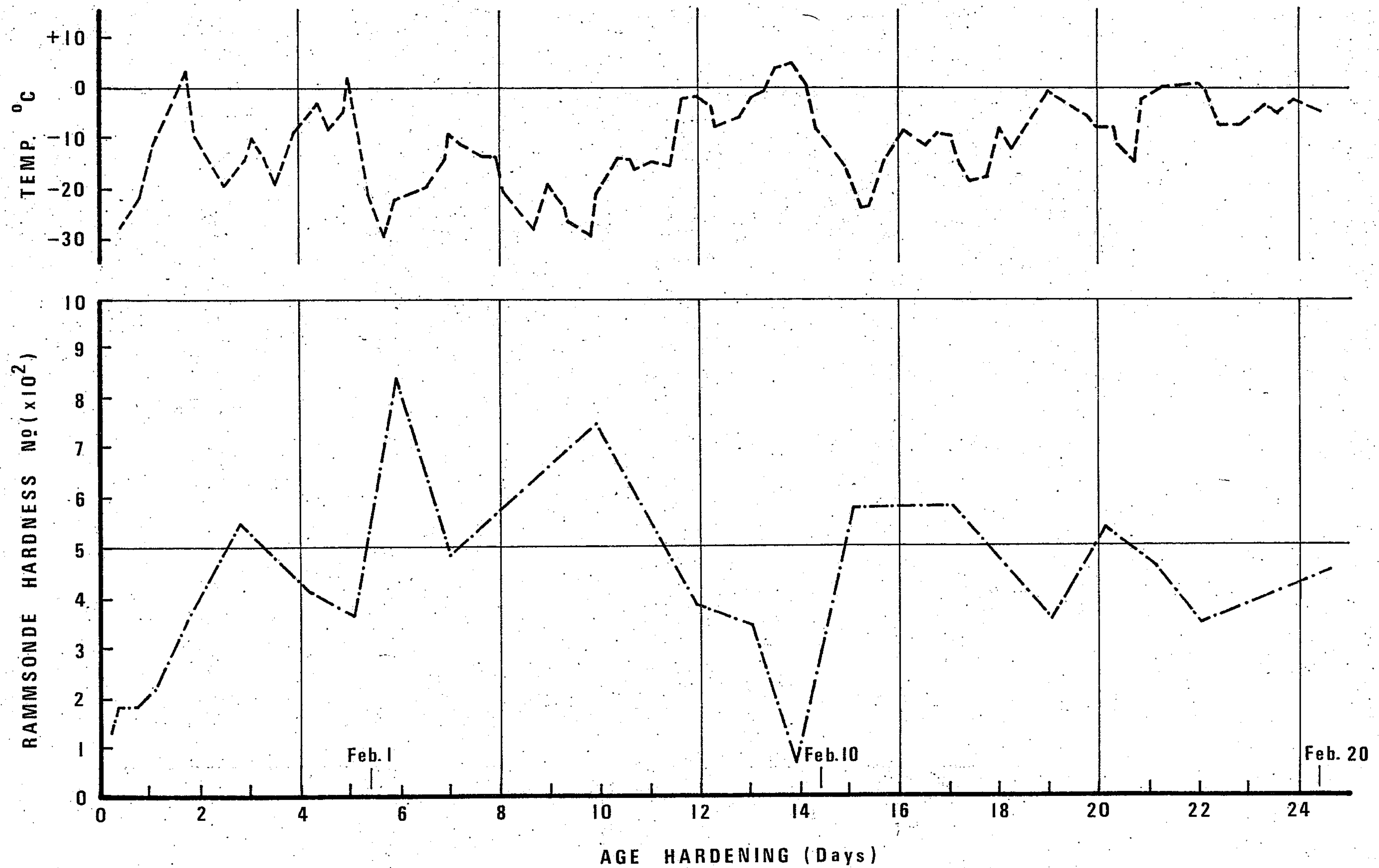

Figure A-2: Relationship between Rammsonde hardness (top 5 cm.), age-hardening time, and air temperature. (Rammsonde hardness values are presented in the corrected form.)

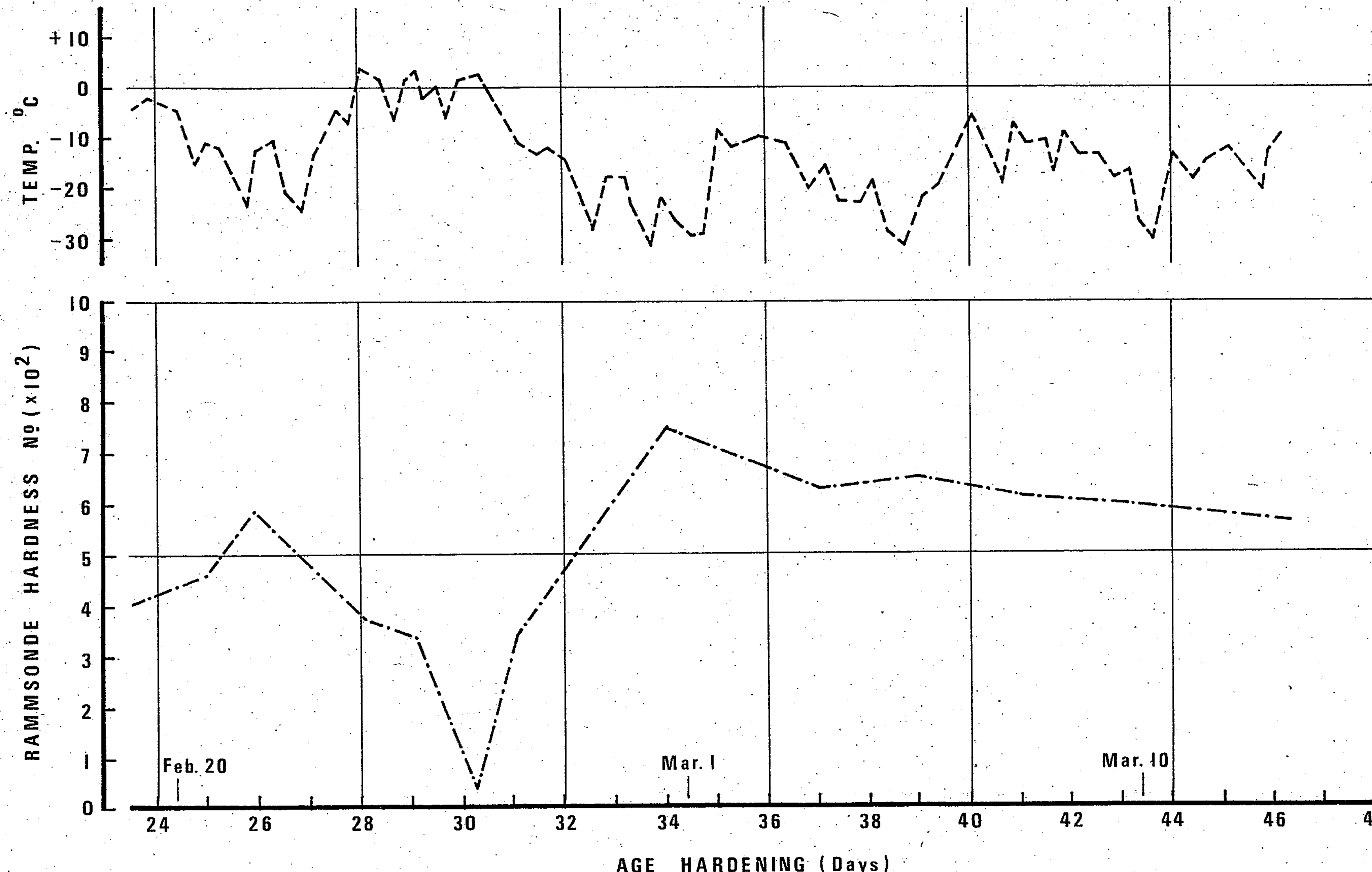

Figure A-2: Continued.

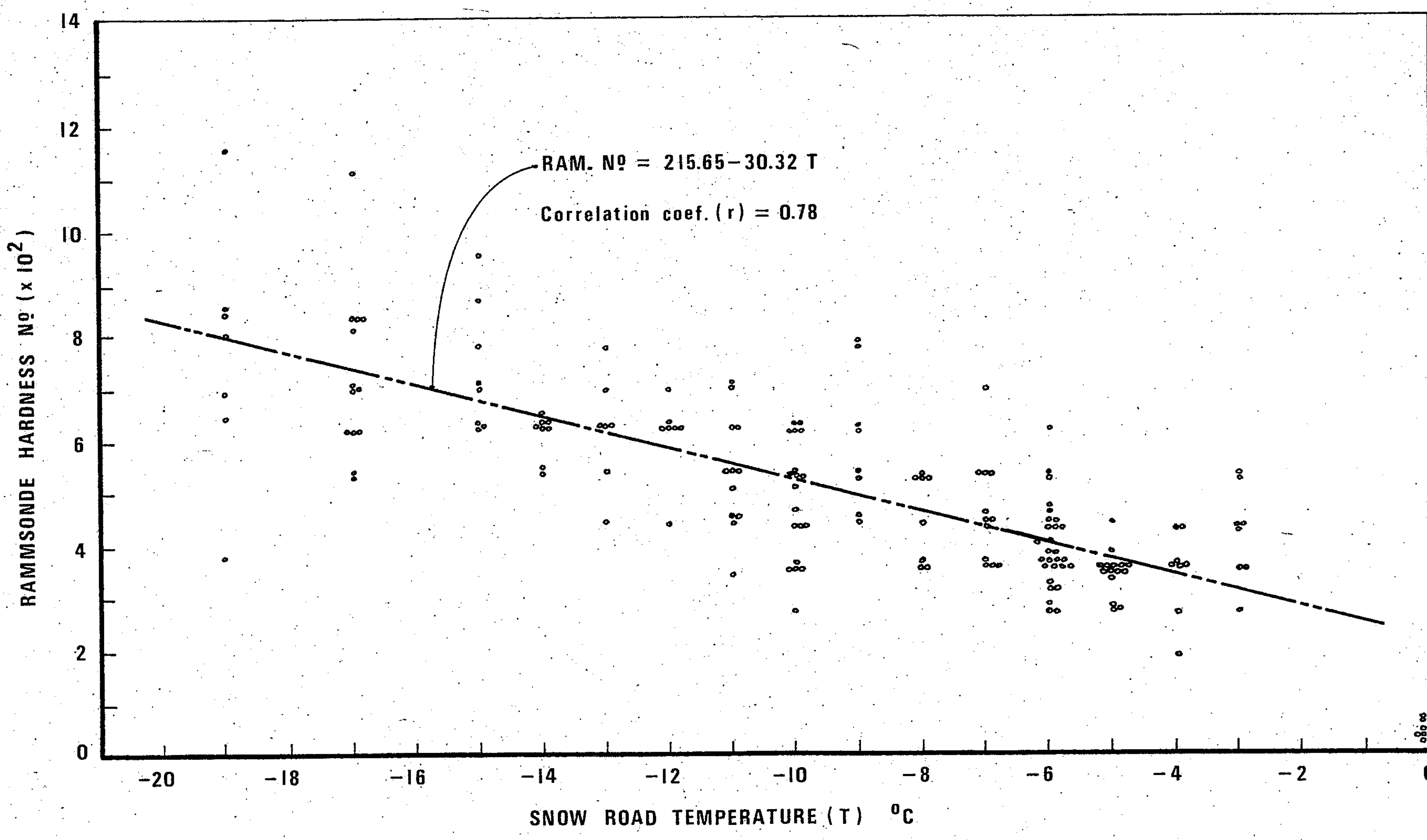

Figure A-3: Scatter diagram of Rammsonde hardness (top 5 cm.) and snow road temperature data. (Rammsonde hardness values are presented in the corrected form.)

TABLE A.3

Average densities of the single- and Multiple-processed snow roads

No. of Blower Passes	Snow-Core Density (gm/cm^3)						Average
1	0.452	0.450	0.454	0.463	0.459	0.471	0.458
2	0.481	0.487	0.489	0.482	0.479	0.471	0.482
4	0.520	0.502	0.532	0.494	0.506	0.512	0.511
6	0.510	0.530	0.508	0.502	0.517	0.506	0.512

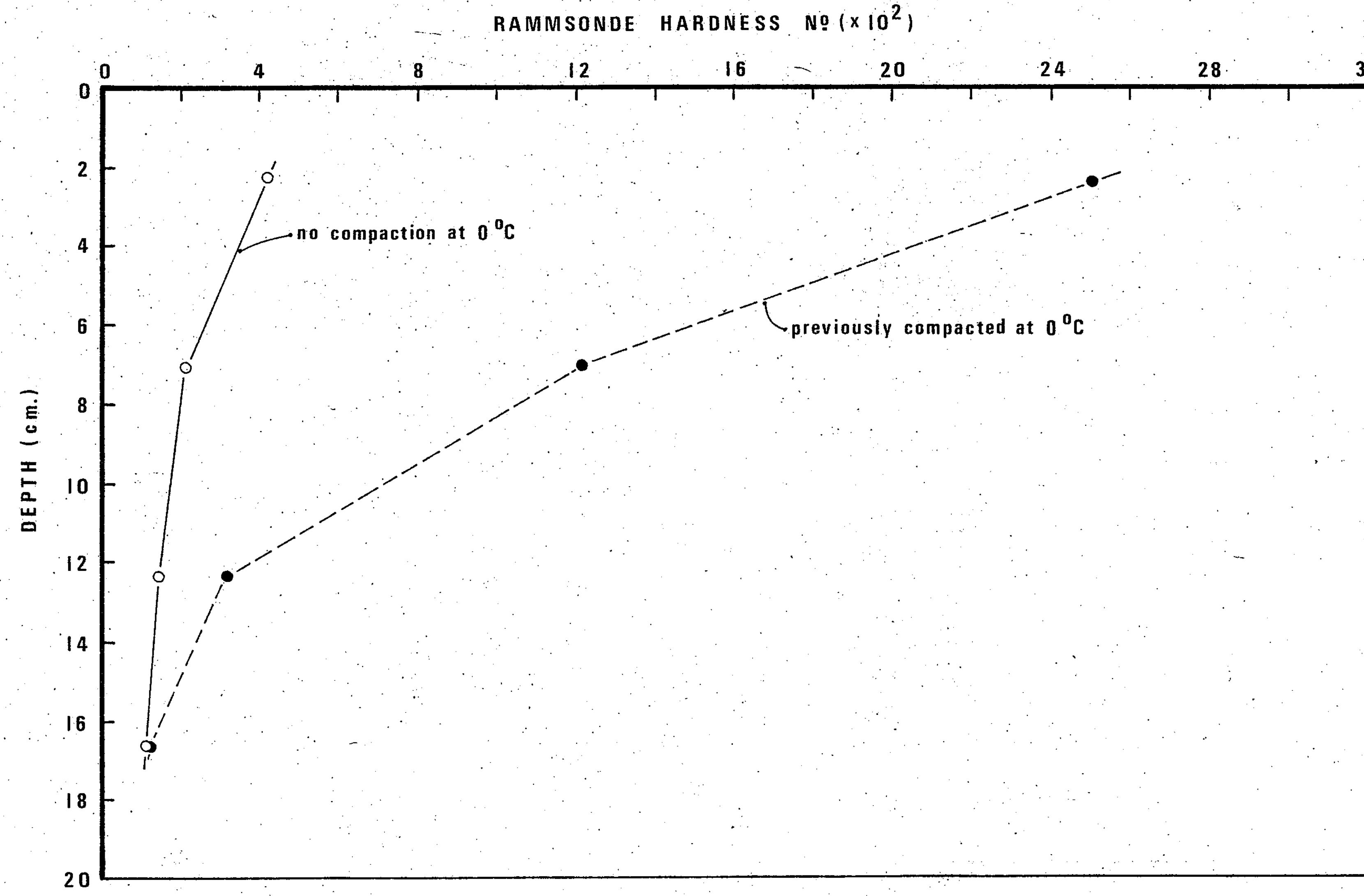

Figure A-4: Typical increase in snow road hardness due to surface compaction at 0°C. (Rammsonde hardness values are presented in the corrected form.)

APPENDIX B

EXPERIMENTAL RESULTS FROM BURN TEST

TABLE B-1

Summary of snow road density profiles before burn test (Mar. 17/76)

Snow Road Density (gm/cm^3)

Core No. \ Depth (cm)	1.5	2.5	5.0	7.5	10.0	12.5	14.0
1	0.535	0.522	0.480	0.525	0.480	0.390	--
2	0.513	0.525	0.510	0.460	0.385	0.360	--
3	0.496	0.525	0.560	0.430	0.425	0.420	--
4	0.485	0.500	0.495	0.450	0.475	0.375	--
5	0.500	0.530	0.530	0.480	0.473	0.360	--
6	0.405	0.510	0.545	0.490	0.425	0.370	--
7	0.481	0.460	0.475	0.463	0.385	0.410	--
8	0.431	0.440	0.515	0.500	0.420	0.410	--
Average	0.481	0.502	0.514	0.475	0.434	0.387	--

TABLE B-2

Summary of snow road density profiles after burn test (Mar. 17/76)

Snow Road Density (gm/cm^3)

Core No. \ Depth (cm)	1.5	2.5	5.0	7.5	10.0	12.5	14.0
1 min. burn							
1	0.550	0.661	0.582	0.600	0.401	0.394	--
2	0.645	0.590	0.545	0.495	0.500	0.450	--
3	0.525	0.600	0.520	0.550	0.520	0.435	--
4	0.565	0.585	0.555	0.670	0.490	0.475	--
5	0.620	0.580	0.525	0.480	0.420	0.380	--
6	0.600	0.580	0.590	0.525	0.455	0.375	--
Average	0.584	0.599	0.553	0.554	0.464	0.418	--
2 min. burn							
1	0.590	0.680	9.585	0.495	0.490	0.440	--
2	0.615	0.630	0.550	0.505	0.500	0.410	--
3	0.550	0.570	0.485	0.455	0.370	0.480	--
4	0.615	0.615	0.570	0.525	0.435	0.475	--
Average	0.593	0.624	0.548	0.495	0.449	0.451	--
4 min. burn							
1	0.640	0.640	0.540	0.435	0.430	0.415	0.315
2	0.620	0.595	0.580	0.535	0.555	0.480	0.455
3	0.475	0.510	0.640	0.585	0.505	0.460	0.370
Average	0.578	0.582	0.587	0.518	0.497	0.452	0.380

TABLE B-2 (continued)

Core No. \ Depth (cm)	1.5	2.5	5.0	7.5	10.0	12.5	14.0
<u>6 min. burn</u>							
1	0.615	0.645	0.600	0.515	0.450	0.415	0.400
2	0.630	0.675	0.625	0.520	0.465	0.490	0.500
3	0.745	0.735	0.450	0.420	0.405	0.345	0.310
4	0.615	0.705	0.660	0.535	0.490	0.415	0.412
Average	0.651	0.690	0.584	0.498	0.453	0.416	0.406
<u>8 min. burn</u>							
1	0.635	0.675	0.590	0.405	0.360	0.415	0.458
2	0.670	0.680	0.585	0.535	0.480	0.460	0.450
3	0.680	0.735	0.700	0.490	0.435	0.380	0.405
Average	0.662	0.697	0.625	0.477	0.425	0.418	0.438
<u>12 min. burn</u>							
1	0.625	0.680	0.580	0.550	0.495	0.450	0.450
2	0.630	0.675	0.495	0.435	0.415	0.360	0.300
3	0.700	0.710	0.680	0.625	0.570	0.525	0.465
Average	0.652	0.688	0.585	0.537	0.493	0.445	0.405
<u>20 min. burn</u>							
1	0.655	0.760	0.645	0.615	0.570	0.525	0.670
2	0.600	0.585	0.590	9.585	0.510	0.450	0.375
3	0.670	0.640	0.515	0.490	9.480	0.415	0.390
Average	0.642	0.662	0.583	0.563	0.520	0.463	0.478

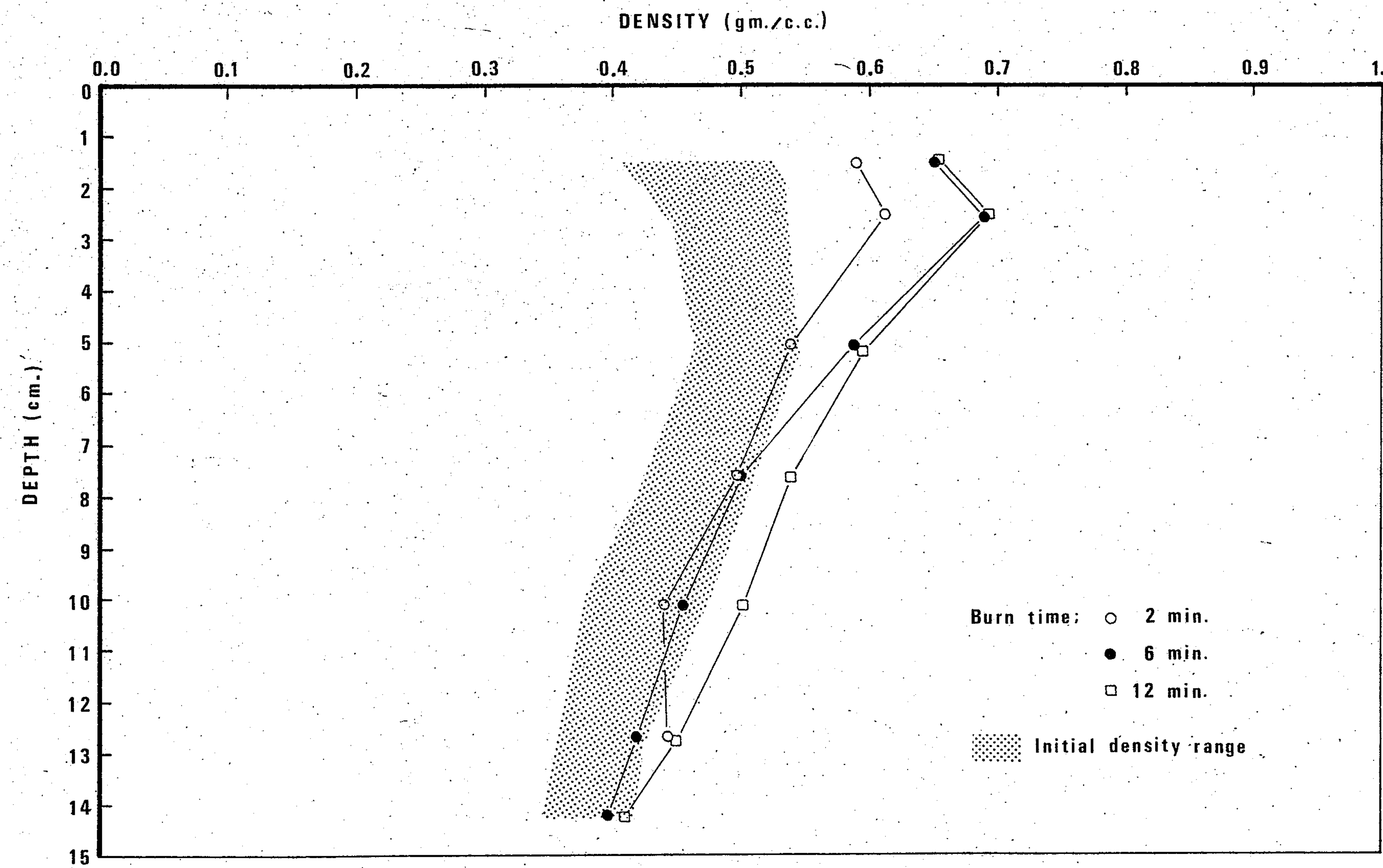

Figure B-1: Snow road density profiles before and after burn tests.

Sample Calculation of Heating Efficiency

General data:

Snow temperature	-9.0°C
Air temperature	-9.0°C
Effective depth of density change	14.0 cm
Thermal value of seasoned pine	8000 Btu/lb
Average burn rate	19 lb/min
Heater/snow contact area	10,000 cm^2
Gross heater output	3,800 $cal/min/cm^2$
Specific heat of snow	0.5 cal/gm/°C
Latent heat of snow	80 cal/gm

The efficiency calculation is based on the average density increase observed in a column of snow road, 1 cm^2 in surface area by 14 cm deep. In this particular calculation, the 6 minute burn interval is considered. This burn interval, for the surface heater used, is equivalent to a forward speed of approximately 1 ft/min. The average density in a snow column 14 cm deep, before and after the burn test (6 min.), was 0.48 gm/cm^3 and 0.55 gm/cm^3 respectively. Therefore, to bring about the density increase, the following heat exchange was required.

(1) Heat required to raise the average snow temperature from -9°C to 0°C;

$$0.5 \text{ cal/gm/°C} \times 0.48 \text{ gm/cm}^3 \times 14 \text{ cm} \times 9\text{°C}$$

$$= 30.24 \text{ cal/cm}^2$$

(2) Density increase (0.48 gm/cm^3 to 0.55 gm/cm^3) is equivalent to the addition of 1 gm of water to the 14 cm column. Thus, the heat required = 80 cal/cm^2.

Therefore by the definition;

$$e = \frac{\text{(Energy theoretically required to achieve the observed density increase)}}{\text{(Total energy expended during the burn interval)}}$$

$$= \frac{30.24 + 80}{3,800 \times 6}$$

$$= 0.005.$$

APPENDIX C

THE RAMMSONDE CONE PENETROMETER

THE RAMMSONDE CONE PENETROMETER

The Rammsonde cone penetrometer consists of a hollow 2 cm-diameter aluminum shaft with a 60° conical probe, a guide rod and a drop hammer. The total length of the standard probe (to the beginning of the shaft) is 10 cm; the cone tip having a diameter of 4 cm and a height of 3.5 cm. The standard Rammsonde penetrometer kit contains two drop hammers, 1 kg and 3 kg in weight. A proper combination of hammer weight and drop height (range 0 to 50 cm) allows a suitable rate of penetration in a variety of snows.

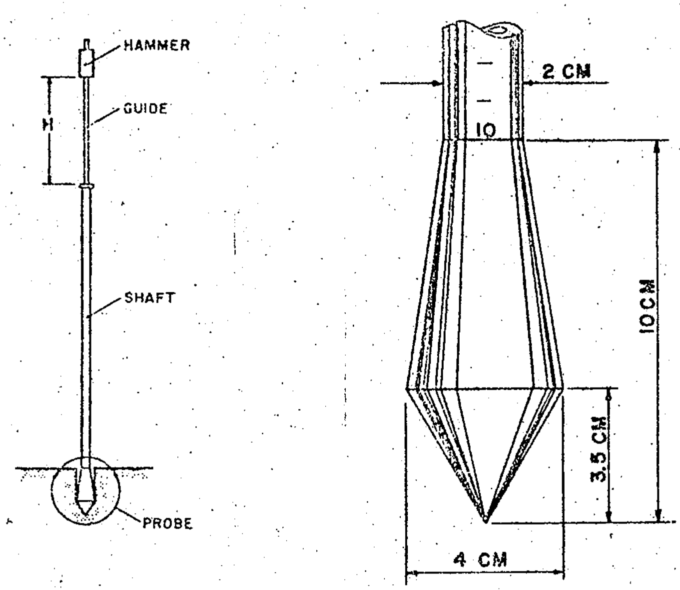

Figure C.1: Diagram of Rammsonde cone penetrometer showing the various components of the instrument.

The hammer is raised by hand to a certain height (H) which is read in centimeters on the guide rod (Fig. C.1) and then dropped freely. The depth of penetration is read from the centimeter scale on the shaft. The resistance to penetration (hardness) of snow can be determined by observing either the amount of the penetration after each hammer drop or the number of hammer drops (blows) necessary to obtain a certain penetration. The hardness reading at any depth, obtained when the tip of the cone is at that depth, represents the mean hardness through the depth increment between this and the previous reading. The Rammsonde hardness is computed from the following expression.

$$R = \frac{WHn}{x} + W + Q \qquad (1)$$

where

R = Rammsonde (ram) hardness number, kg.,

W = weight of drop hammer, kg.,

H = height of drop, cm.,

n = number of hammer blows,

x = penetration after 'n' blows, cm., and

Q = weight of penetrometer, kg.

Equation (1) is a simplification of the real case and is not completely satisfactory for every situation encountered. Re-evaluation of the equation by Bender, Brunke and Niedringhaus (Veda, Sellman and Abele [37]) has shown that because of the conical shape of the penetrometer head and the proximity of a free surface, the resistance number obtained requires correction. The resistance number (R), for the 0 to 5 cm depth has to be multiplied by 4.7, that for the 5 to 10 cm depth by 1.6, or that for the 0 to 10 cm depth by 3.0. It has not been standard practice, however, to apply these corrections, and therefore, the ram hardness data and correlations to the strength parameters as presented in the literature, are generally in the uncorrected form. A further limitation of the Rammsonde cone penetrometer in its present shape, is that it becomes unreliable as an indicator when hardness values exceed 800 kg.

Although R has units of kilograms, the magnitude of R, except in relative terms, has no real significance. The following review of Rammsonde hardness equations will serve to illustrate the rather arbitrary nature of equation (1) and its limitations.

<u>The Original Rammsonde Hardness Equation</u>

The original ram hardness equation was developed by reasoning that the kinetic energy of the falling hammer equals the mean force R, times the penetration S. That is;

$$RS = \frac{WV_1^2}{2g} \tag{2}$$

where

W = weight of hammer,

V_1 = velocity of hammer upon impact,

S = penetration into the snow, and

g = gravitational constant.

By substituting the identity,

$$\frac{1}{2}\, m\, V_1^2 = m\, gH \tag{3}$$

where

m = mass of hammer, and

H = height of hammer fall.

into equation (2), the original equation was derived as

$$R = \frac{WH}{S} \; . \tag{4}$$

Equation (4) proved unsatisfactory as the impact effect is not accounted for. That is, W is not the weight and V_1 is not the velocity of the system in motion during the penetration. It is interesting to note, however, that the right hand side of equation (4) is also the first term in equation (1).

Niedringhaus equation for ram hardness

The momentum of the system after impact was accounted for in the following way. In order to conserve momentum, it was assumed that,

$$W\, V_1 = W_T V_2 \tag{5}$$

where

W_T = total weight = W + Q,

Q = weight of penetrometer, and

V_2 = common velocity after impact, of the penetrometer and hammer.

The kinetic energy of the system, following the impact of the hammer is therefore,

$$RS = \frac{W_T V_2^{\ 2}}{2g} \;. \tag{6}$$

Substituting V_2 of equation (5) into equation (6) gives;

$$RS = \frac{W_T W^2 V_1^{\ 2}}{2gW_T^2} \tag{7}$$

and since

$$V_1^2 = 2gH \tag{3}$$

equation (7) becomes

$$R = \frac{WH}{S} \cdot \frac{W}{W_T} \tag{8}$$

Equation (8) (Niedringhaus equation) was evaluated as follows (Waterhouse [41]): Since a common velocity for the penetrometer and hammer (after impact) was assumed, the collision is treated as inelastic. Later tests showed that this assumption was not valid and that R varied considerably with changes in hammer weight. Equation (8) was consequently discarded.

Haefeli ram hardness equation

In an attempt to correct the Rammsonde hardness equation deficiencies, Haefeli (1963) developed an equation that included the coefficient of restitution for the hammer-penetrometer collision. The ram hardness was expressed as;

$$R = \frac{WH}{S} \cdot \frac{W + e^2 W_T}{W + W_T} \tag{9}$$

where

e = coefficient of restitution, and

Other symbols as previously defined.

As with equation (8), Haefeli's equation could not be generally applied as it too was sensitive to variation in hammer and total weight.

Hiley ram hardness equation

The Hiley equation is based on pile driving technology and (in the present nomenclature) is written as:

$$R = \frac{WH}{S} \cdot \frac{W + e^2 Q}{W + Q} \tag{10}$$

Comparing to equation (9) we can see that W_T was replaced by Q.

Waterhouse [41] indicates that utilization of equation (10) for the ram number would permit future correlation over a broad range of materials and conditions.

As was evidenced in the review, the limitations of the dynamic formulae result from the inability to account for energy losses during cone penetration. Since accountability of all losses is impossible, a certain margin of error is inevitable.

APPENDIX D

DETERMINATION OF SNOW DENSITY USING A RADIATION MEASUREMENT TECHNIQUE

DETERMINATION OF SNOW DENSITY USING A RADIATION MEASUREMENT TECHNIQUE

Equipment and Materials Used

1 Nuclear-Chicago, Model 8775, scaler/timer

Scaler: - 5 decade readout
- 99999 maximum count capacity
- preset count capability

Timer: - 4 decade readout
- 99.99 minutes maximum time capacity
- preset time capability

1 Harshaw, Model DS-200, crystal scintillation detector

Crystal: -sodium iodide, thallium, activated, NaI(Tl)
- 2 in-diameter by 2 in-thick
- resolution better than 10% (Nuclear-Chicago Corp. [33])

1 Cobalt-60, 1 milli-curie gamma-ray source

Machined lead brick shielding

Equipment Setup and System Characteristics

The scintillation detector was aligned and set 12 cm away from the face of the lead shielding, thus making the distance to the radioactive source 17 cm (see Figure D.1). The equipment, in this configuration, had the following characteristics.

1) System efficiency - The "system efficiency" was defined by the relationship;

$$e = \frac{CPM - BPM}{DPM} \tag{1}$$

where

e = system efficiency,

CPM = recorded counts per minute,

BPM = background count per minute determined when all radioactive sources were removed from the vicinity of the detector, and

DPM = disintigration per minute of the radioactive source (1 curie = 3.7×10^{10} disintegrations per second).

For the present system, where a 1 milli-curie gamma-ray source was used, the efficiency was 0.015%. Also throughout the tests, BPM was always less than 2% of CPM. The low system efficiency is due to the high absorption of the gamma radiation within the lead shielding.

2) Coincidence loss - Because of the random nature of emissions from a radioactive sample it is possible for a particle emission to enter the detector while the detector is still "paralized" from a previous pulse. Incorrectly, in this case, only one pulse would be detected by the counting system. The significance of this counting error depends on the resolution time of the detector. The correction for this source of error is reasoned as follows.

$$t = \frac{CPM\ (T)}{60} \tag{2}$$

where

t = time in minutes during which the system is insensitive per each 1-minute count interval,

CPM = recorded counts per minute, and

T = the resolution time of the detector in seconds.

Since there is as much chance for emissions to occur during time 't' as during any other period of equal duration,

$$\% \text{ of counts lost} = \frac{\text{CPM}(T)}{60} \times 100 \qquad (3)$$

and therefore

$$\text{number of counts lost per minute} = \text{CPM} \times t \quad . \qquad (4)$$

Testing Procedure

The snow core samples were positioned midway between the lead shielding and detector on an adjustable stand which could be elevated or lowered as desired. A minimum of 10 counts of 0.2 minute duration were made at each point (spaced from 1.0 to 2.5 cm apart) along the length of the core. The count/density relationship for the snow was assumed to be linear and the slope of the relationship was determined from the average count for a container filled with water and that for the empty container. The inside diameter of the plastic container (5 cm) was the same as the outside diameter of the snow core samples. Having accounted for the loss in recorded count due to the plastic container, a chart for the count/density relationship was developed. Prior to each round of testing, however, the chart was corrected for fluctuation in background noise. Furthermore, all recorded counts were corrected for coincidence loss as described by equation (4).

Statistical Interpretation of Data

The 10 counts of 0.2-minute duration at each point along the core were each treated as random samples of a larger population. The sample mean (m_s) was computed and assuming a normal distribution for the count rate, the standard deviation for the sample was calculated. Over 250, 10-count samples were obtained and in every case the standard deviation was less than 1% of the sample mean. The result could be expressed as "$m_s \pm 1\%$ at 68.3% probability".

To estimate the population mean (m_p), however, the error associated with the mean value determined from a sample of random counts must be considered. The error is inversly proportional to the square root of the total number of counts (regardless of the time required) and is expressed as follows:

$$\text{error} = \frac{k}{\sqrt{n}} \tag{5}$$

where

k = a measure of confidence, and

n = number of counts observed.

If k is expressed in terms of "number of standard deviations" from the sample mean, than the deviation that is statistically expected in the sample mean is;

$$\% \text{ deviation} = \frac{k}{\sqrt{n}} \times 100 \tag{6}$$

where

k = confidence constant (expressed as "number of standard deviations" from the sample mean), and

n = number of counts observed.

Choosing $k = 1$ as the required confidence, and for $n = 10$, the statistical error in m_s as an approximation of m_p, is 32%. That is, there is a 68.3% probability that the population mean (m_p) falls within the range $m_s \pm$ 32%. To reduce the statistical error, the sample size would have to be increased. For example, for a 68.3% probability ($k = 1$) that m_p would fall within the range $m_s \pm 10\%$, the sample size 'n' would have to be 100.

In the tests described, a small sample size (10 counts of 0.2-minute duration each) was necessarily chosen as the testing facilities were not temperature controlled. With a larger sample size, significant melting of the snow would have occurred.

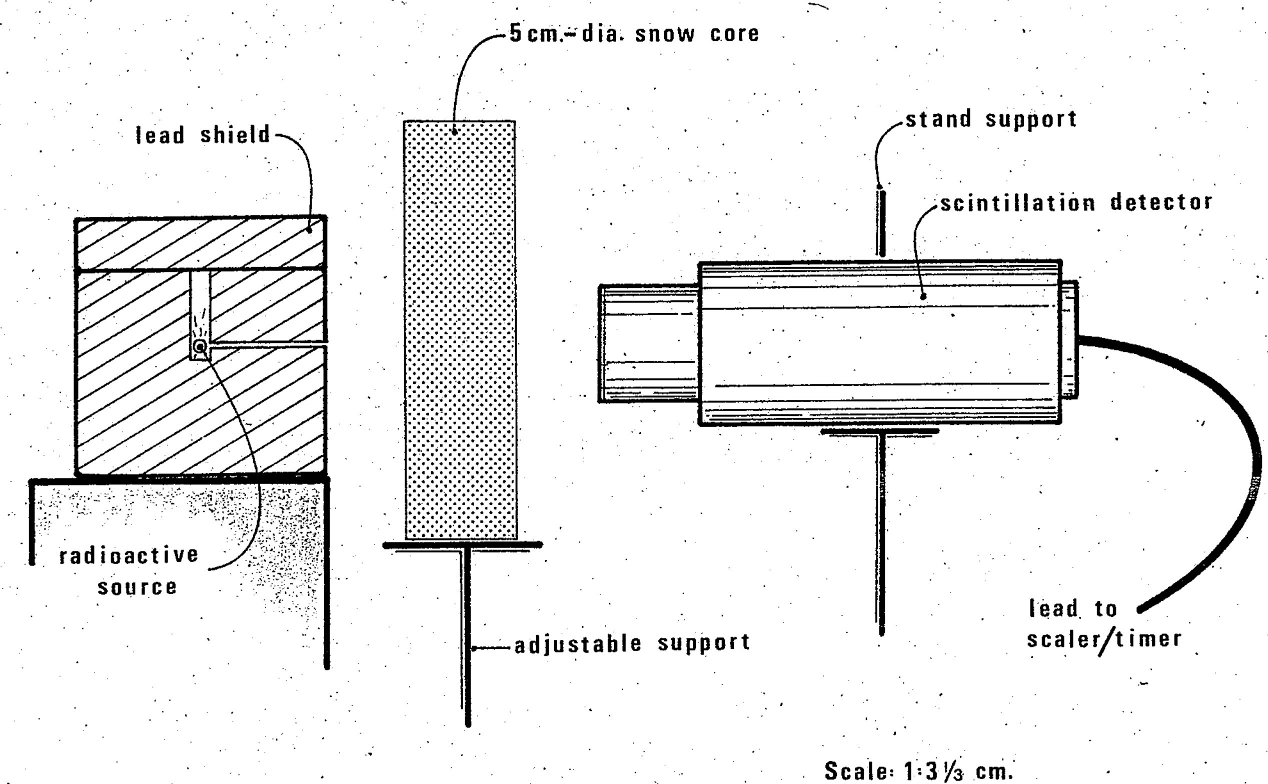

Figure D-1: Diagram showing the arrangement and basic components of the radiation/scintillation apparatus.

APPENDIX E

CONSTRUCTION EQUIPMENT AND MATERIALS

DESCRIPTION OF CONSTRUCTION EQUIPMENT AND MATERIALS

Champion motor grader, Model D-562D

Weight:	26,495 pounds
Engine:	672 cu. in. Cummins diesel
Width:	7 feet 9 inches
Turning radius:	40 feet
Tires:	14.00 x 24, 12 ply
Tire pressure:	20 psi

Allis-Chalmers (loader) tractor, Model TL14D

Engine:	Model 6000 diesel
Transmission:	Power shift
Cab:	Industrial cab Model 8266
Tires:	14.00 x 24, 12 ply
Tire pressure:	20 psi

TL14D tractor equipped with Sicard snow blower and IHC power unit.

Sicard snow blower "Snowmaster Baby", Model BMG4-27

Blower frame:	3/16 in.-thick plate steel intake hood, 78 in. wide and 30 in. high mounted on 3 - 1/2 in. thick steel skates.
Conveyor assembly:	2 - 25 in. diameter, 3/16 in.-thick steel augers. Left and right auger

	sections welded at center to form impeller
Discharge chute:	Casting direction variable 180° with 10 to 50 foot casting distance capability.
Clutch:	Twin disc
Engine R.P.M. reduction gear box:	3.6:1 gear ratio

<u>IHC snow blower power unit, Model UV-345</u>

Engine:	8 cylinder, 3 7/8 in. bore, c 21/32 in. stroke
Full load R.P.M.:	2500 ± 100

<u>J.I. Case loader, Model 1150</u>

Engine:	6 cylinder 451 c.i.d. case diesel
Operating weight:	approximately 24,000 lb with bucket and counterweight
Track:	15 inches wide, ground pressure (approx.) 9 psi.

<u>Steel roller, Enterprise Mfg. Co.</u>

Diameter:	4 feet 2 inches
Width:	4 feet 4 inches
Weight:	approximately 2 tons

Steel I-beam drag

Cross-section:	W10 x 29
Length:	11 feet
Weight:	320 lbs.

Seasoned pine fire-wood

Quantity used:	1 cord
Wood density:	27 lb/ft^3
Volume of solid wood per cord:	85 ft^3
Weight per cord:	2295 lb.
Thermal value:	8000 Btu/lb.
Average burning rate during burn test:	19 lb/min.

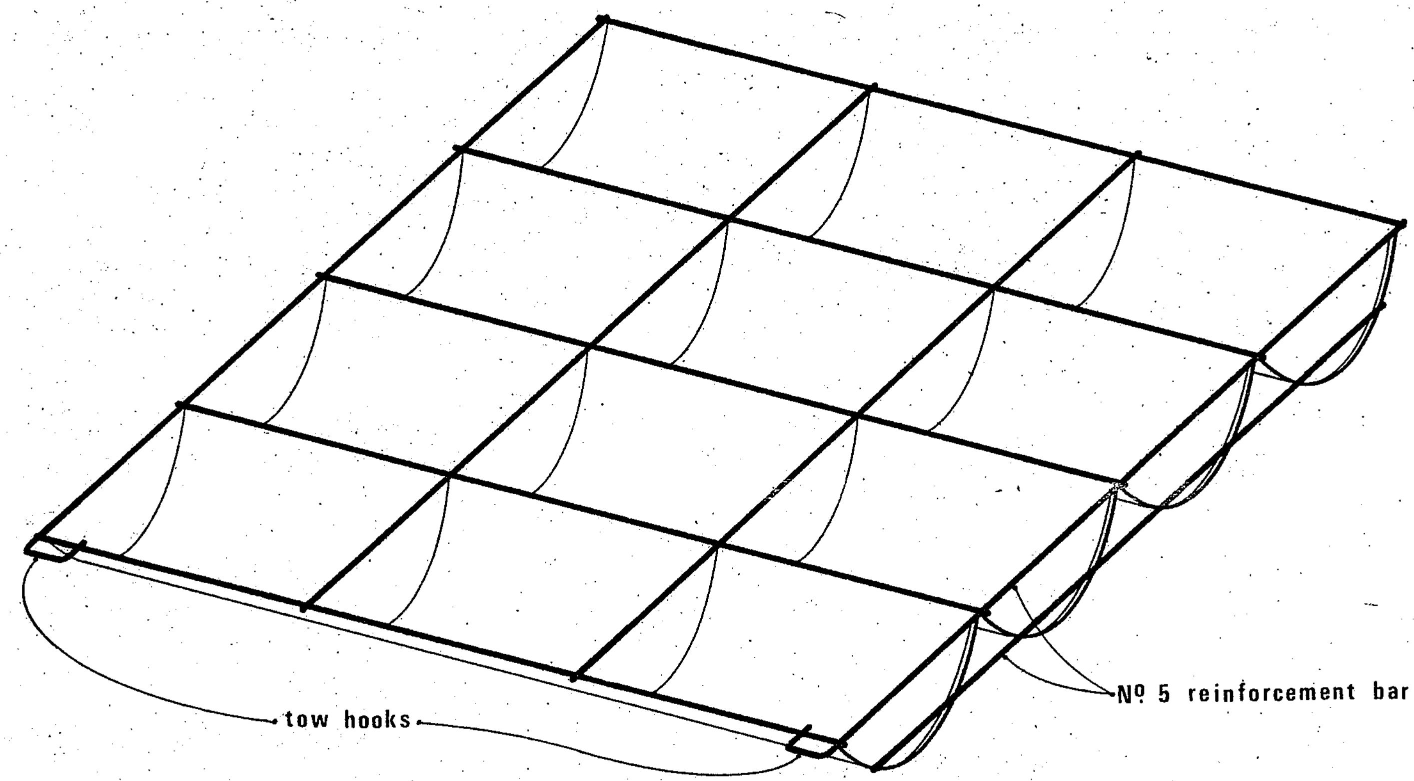

Figure E-1: Diagram showing the construction of the prototype wood-fired surface heater. (Six, 45 gal , oil drums are cut and welded together as shown.)

Photograph E-1: Windrowing the snow with the Champion motor grader in preparation for processing with the Sicard snowblower.

Photograph E-2: A view of the snowblower/tractor unit processing the windrowed snow and depositing it along the proposed roadway.

Photograph E-3: The roadway after final snow processing and deposition. (Note: Photo. E-3 illustrates the spreading capability of the Sicard snowblower. The snow depth varies from 1.5 go 3.0 feet).

Photograph E-4: Road surface after leveling and dragging with the steel drag.

Photograph E-5: Station-wagon traveling over snow road with no detrimental effect on road surface. (Tire inflation pressure 28 psi.)

Photograph E-6: The Champion motor grader blading minor snow accumulation from the snow road surface.

Photograph E-7: The prototype surface heater shown fully fueled with one (1) cord of seasoned pine.

Photograph E-8: A view of the surface heater in operation. (Note trail of ash and cinders on road surface.)